ELSEVIER

Contents lists available at ScienceDirect

Computers and Chemical Engineering

journal homepage: www.elsevier.com/locate/compchemeng



Integrated process design, scheduling, and control using multiparametric programming



Baris Burnak^{a,b}, Nikolaos A. Diangelakis^{a,b}, Justin Katz^{a,b}, Efstratios N. Pistikopoulos^{a,b,*}

- ^a Artie McFerrin Department of Chemical Engineering, Texas A&M University, College Station, TX 77845, USA
- ^b Texas A&M Energy Institute, Texas A&M University, College Station, TX 77845, USA

ARTICLE INFO

Article history: Received 7 December 2018 Revised 1 March 2019 Accepted 2 March 2019 Available online 14 March 2019

Keywords:
Enterprise-wide optimization
Integration
Multi-parametric programming
Process scheduling
Model predictive control
Process design

ABSTRACT

A unified theory and framework for the integration of process design, control, and scheduling based on a single high fidelity model is presented. The framework features (i) a mixed-integer dynamic optimization (MIDO) formulation with design, scheduling, and control considerations, and (ii) a multiparametric optimization strategy for the derivation of offline/explicit maps of optimal receding horizon policies. Explicit model predictive control schemes are developed as a function of design and scheduling decisions, and similarly design dependent scheduling policies are derived accounting for the closed-loop dynamics. Inherent multi-scale gap issues are addressed by an offline design dependent surrogate model. The proposed framwork is illustrated by two example problems, a system of two continuous stirred tank reactor, and a small residential combined heat and power (CHP) network.

© 2019 Elsevier Ltd. All rights reserved.

1. Introduction

The complexity of decision making problems in the process industry has conventionally resulted in isolation of decisions with respect to the time scales of their effects on the operation, ranging from years-spanning supply chain management to seconds-long process control decisions. The isolated layers are structured hierarchically, as shown in Fig. 1a, with an information flow allowed dominantly in descending order in the time scales they span. However, independent and sequential assessment of the decision layers leads to suboptimal, even infeasible operations. Integration of these layers across an enterprise is expected to deliver more profitable and reliable operations by benefiting from the synergistic interactions between different decisions (Grossmann, 2005). Recent advances in operational research and rapid decrease in the cost of computational hardware provide an opportunity for the academia and the industry to seek a tractable and systematic methodology for simultaneous consideration of multi-scale decisions (Pistikopoulos and Diangelakis, 2016). However, seamless integration of decision layers at different time scales and objectives is still an open question due to the high dimensionality and complexity of each constituent problem, such that process systems en-

E-mail address: stratos@tamu.edu (E.N. Pistikopoulos).

gineering tools and perspectives can play a key role for a holistic solution (Daoutidis et al., 2018).

Process design decisions, such as equipment selection and sizing, span the widest time-scale in the functional hierarchy of a chemical process, and they are typically established by solving a steady-state design optimization problem (Rafiei and Ricardez-Sandoval, 2018). Operational decisions such as scheduling and control are usually assumed to take a nominal value to make the problem complexity tractable (Nie et al., 2015). However, rapidly changing market conditions and process disturbances often force the system to operate under a wide range of operating conditions, which may render the steady-state process design dynamically infeasible. Design optimization under such operational uncertainties have been extensively investigated in the literature by considering feasibility, flexibility, stability, controllability, and resilience metrics (Diangelakis et al., 2017b; Pistikopoulos and Ierapetritou, 1995; Ricardez-Sandoval, 2012b). An indicative list of contributions towards the integration of operational decisions in the design optimization problem is presented in Table 1. Similar to process design, operational decisions including production sequence, transition, allocation of tasks in multiple units are optimized with limited consideration of the physical process dynamics. Overlooking these fast dynamics while making longer term economical decisions creates an inherent mismatch between the operational set points determined by the scheduler and the closed loop performance governed by the control strategy (Baldea et al., 2015; Burnak et al., 2018b). These inherently different domains of the

 $^{^{\}ast}$ Corresponding author at: Texas A&M Energy Institute, Texas A&M University, College Station, TX 77845, USA.

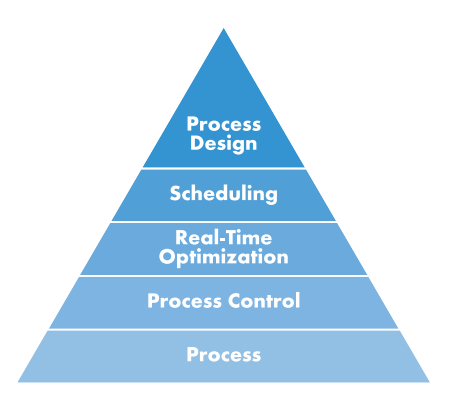
Table 1Design, scheduling, and control in the literature: An indicative list.

Author (year) Design & control	Contribution
Narraway et al. (1991), Soroush and Kravaris (1993b), Soroush and Kravaris (1993a), Papalexandri and Pistikopoulos (1994), Mohideen et al. (1997), Luyben and Floudas (1994), Floudas (2000); Floudas et al. (2001), Bahri et al. (1997), Chatrattanawet et al. (2014), Gong et al. (1995), Vega et al. (2014a)	Feasibility, flexibility, stability, controllibility, resilience metrics in steady-state design optimization with MIDO or MINLP
Bansal et al. (2000a), Bansal et al. (2000b), Bansal et al. (2002), Georgiadis et al. (2002), Bansal et al. (2003), Sakizlis et al. (2003), Sakizlis et al. (2004), Malcolm et al. (2007), Washington and Swartz (2014), Ricardez-Sandoval (2012a)	Integrated MIDO formulation/ decomposition with PID control or (mp)MPC
Flores-Tlacuahuac and Biegler (2007), Flores-Tlacuahuac and Biegler (2008), Brengel and Seider (1992), Ricardez-Sandoval et al. (2008), Mehta and Ricardez-Sandoval (2016), Rafiei-Shishavan et al. (2017), Mohideen et al. (1996), Kookos and Perkins (2002), Kookos and Perkins (2016), De La Fuente and Flores-Tlacuahuac (2009), Chen et al. (2011a), Chen et al. (2011b), Li and Barton (2015), Zhang et al. (2006)	Iterative MINLP formulation with stochastic back-off formulation for uncertainty
Ghobeity and Mitsos (2014); Ricardez-Sandoval (2011); Ricardez-Sandoval et al. (2009); Vega et al. (2014b); Yuan et al. (2012)	Review articles on design and control integration
Scheduling & control	
Flores-Tlacuahuac and Grossmann (2006), Terrazas-Moreno et al. (2007), Flores-Tlacuahuac and Grossmann (2010), Flores-Tlacuahuac and Grossmann (2011), Gutiérrez-Limón et al. (2012), Gutiérrez-Limón et al. (2014), Mitra et al. (2010), Nie et al. (2012), Nie et al. (2015), Capón-García et al. (2013), Chu and You (2013), Pattison et al. (2016), Kelley et al. (2018)	Decomposition of MIDO or MINLP and open loop optimal control
Chatzidoukas et al. (2003); Chu and You (2012); Costandy et al. (2018); Du et al. (2015); Mahadevan et al. (2002); Zhuge and Ierapetritou (2012)	Formulation/ Decomposition of MIDO schedule with PID control
Zhuge and Ierapetritou (2014), Dias et al. (2018), Ellis and Christofides (2014b), Ellis and Christofides (2014a), Ellis and Christofides (2015), Alanqar et al. (2017), Baldea et al. (2015), Dias et al. (2018), Jamaludin and Swartz (2017), Diangelakis et al. (2017a), Burnak et al. (2018b), Charitopoulos et al. (2018), Beal et al. (2018)	(mp)MPC implementation in economic receding horizon policies
Huercio et al. (1995), Würth et al. (2011), Amrit et al. (2011), Subramanian et al. (2012), Subramanian et al. (2013), Kopanos et al. (2013), Kopanos and Pistikopoulos (2014), Touretzky and Baldea (2014), Liu and Liu (2016)	Control theory/ Economic MPC in scheduling problems
Bassett et al. (1996), Grossmann (2005), Harjunkoski et al. (2009), Engell and Harjunkoski (2012), Baldea and Harjunkoski (2014), Ellis et al. (2014), Chu and You (2015), Dias and Ierapetritou (2016), Dias and Ierapetritou (2017)	Review articles on scheduling and control integration
Design, scheduling & control	
Patil et al. (2015); Terrazas-Moreno et al. (2008) Koller et al. (2018) Burnak et al. (2018a)	Formulation of MIDO and open loop control under uncertainty PI control and stochastic back-off approach for uncertainty Explicit, design dependent optimal rolling horizon strategies

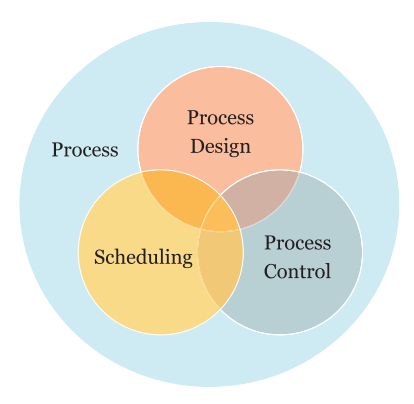
design, scheduling, and control decisions are illustrated in Fig. 1b. Any decision that lies outside the intersection of all layers results into an inoperable point, where at least one of the layers fails to find a feasible decision.

Integrated approaches aim to systematically assess the tradeoffs between different decision layers by reconstructing the problems into a unified formulation. The reformulated problem augments the feasible space of operation by simultaneously considering the degrees of freedom of the constituent problems, enabling more cost effective and reliable decisions. Although such monolithic approaches deliver the expected benefit of integration (Flores-Tlacuahuac and Grossmann, 2006; 2010; Zhuge and Ierapetritou, 2012; 2014), they are susceptible to process disturbances and changing demands. The discretization and reformulation steps result into a large scale non-convex mixed-integer nonlinear programming (MINLP) problem that is computationally taxing to solve online after every disruptive event (Engell and Harjunkoski, 2012). A low-order representation of the high-fidelity model (Du et al., 2015) and decomposition techniques (Chu and You, 2012) have been two fundamental approaches to acquire tractable and fast solutions to this challenging problem. An indicative list of contributions to integrate scheduling and control layers is presented in Table 1.

Model Predictive Control (MPC) has been shown to be a useful tool for process automation with its capabilities to handle complex interactions between multiple process outputs and multiple manipulated actions (MIMO systems), to satisfy dynamic physical and operational constraints, and to predict the future outcomes of the process (Qin and Badgwell, 2003). Despite these advantages, integration efforts using an MPC strategy is limited in the literature due to the implicit nature of the control structure. The necessity to formulate an optimization problem at every sampling time under a longer time scale decision layer significantly increases the overall problem complexity, making explicit control structures such as PID controllers more suitable for integration purposes. However, multiparametric programming allows for an exact offline solution of an MPC problem (referred as explicit MPC or mpMPC) as a piecewise affine function of bounded parameters, including initial conditions, output set points, input reference trajectories, and operational bounds (Bemporad et al., 2002). Although there have been successful implementations of mpMPC in design optimization (Diangelakis et al., 2017b), and scheduling (Burnak et al., 2018b; Zhuge and Ierapetritou, 2014), a simultaneous integration of design, scheduling, and control with explicit maps of rolling horizon strategies has never been attempted in the open literature.



(a) Hierarchical approach.



(b) Integrated approach.

Fig. 1. Decision making layers in an enterprise.

In this study, we present a novel framework to integrate design, scheduling, and control problems by deriving explicit maps of optimal decision making strategies at both levels of operation based on a single high fidelity model. We explicitly map the upper level layer decisions on the lower levels by multiparametric programming. The explicit expressions at the lower level layers enable their representation in the upper level problems. In other words, the control problem is derived as a function of design and scheduling decisions, and similarly the scheduling decisions are design dependent, and aware of the controller dynamics. These explicit scheduling and control maps allow for an exact implementation in a design optimization problem. Furthermore, we introduce a design dependent surrogate model formulation to bridge the time scale gap between the schedule and the control problems, which is also solved offline. Direct inclusion of operating strategies in the design optimization ensures the process operability by enforcing the decisions to be selected from the intersection of all layers from

The remainder of the paper is organized as follows. Section 2 defines the integration problem that is addressed in this study, and describes the proposed framework to approach the problem. The framework is showcased in Section 3 on systems of reactors and residential combined heat and power (CHP) units. Lastly, Section 4 presents concluding remarks and future directions.

2. Integration of design, scheduling, and control via multiparametric optimization

In this section, we define the extent of the integrated problem, provide the mathematical representation of the considered problem formulation, and introduce the tools and the framework to deliver the targeted objectives.

2.1. Problem definition

We consider a generic process where the interactions between the long term (design), middle term (schedule), and short term (control) decisions are sufficiently significant to impact the feasibility and the optimality of each individual decision. Therefore, we define the following problem that encapsulates all three decisions simultaneously.

- (i) Given: A high fidelity model based on first principles or data-driven modeling techniques that accurately captures the dynamics of the system, any physical limitations of the system due to process safety considerations or product specifications, unit costs for design, raw material, energy, and inventory, revenue for unit product, and an accurate demand forecast.
- (ii) Determine: Production sequence throughout an operating horizon, closed loop control strategy that delivers the product specifications, set points for the operation tailored for the dynamics of the closed loop strategy, size of the processing equipment that ensures operability of the process.
- (iii) Objective: Minimize the operating and capital costs.

Note that the objective of the problem can be replaced by the minimization of the energy utilization, CO_2 emissions, processing time, or a combination of these tasks based on the application without changing the framework. In this study, we showcase the minimization of costs as it is the most frequently used objective in process operations.

2.2. Problem formulation

A generalized mathematical representation of the simultaneous design, scheduling, and control problem introduced in Section 2.1 is given by Eq. (1) in the form of a mixed integer dynamic optimization (MIDO) problem.

$$\min_{\substack{u,s,des}} J = \int_0^{\tau} P(x, y, u, s, des, d) dt$$

$$s.t. \quad \dot{x} = f(x, u, s, des, d)$$

$$\underline{y} \le y = g(x, u, s, des, d) \le \overline{y}$$

$$\underline{u} \le u = h(x, u, s, des, d) \le \overline{u}$$

$$\underline{s} \le s = m(x, u, s, des, d) \le \overline{s}$$

$$x \le x \le \overline{x}, \quad des \le des \le \overline{des}, \quad d \le d \le \overline{d}$$

$$(1)$$

where x are the states of the system, y are the system outputs, u are the control actions, s are the scheduling decisions, des are the design variables, and d are the measured disturbances, P is the cost function accounting for the operating and capital costs, f and g are differential and algebraic relations, h and m are the implicit relations that describe the operational decisions, and lower and upper bars are the bounds on the variables. We also differentiate the disturbances at the control level, $d^c \subseteq d$, such as the variations in the feed conditions, and the disturbances at the scheduling level, $d^s \subseteq d$, such as the fluctuating market prices and demand rates. Note that discrete design and scheduling decisions such as the number of trays in a distillation column and the product to be manufactured at a particular time instance render Problem 1 a mixed-integer optimization problem.

The problem definition detailed in Section 2.1 states that the high fidelity model given by f and g, the cost function P, the bounds on the variables are known, and a realistic demand scenario is available. The goal is to minimize the objective P over a

time horizon τ by manipulating the degrees of freedom of the system available in the long term (*des*), middle term (*s*), and short term (*c*).

The significantly distinct time scales of the manipulated variables yield a large scale MIDO problem that is computationally intractable by the established approaches such as the direct, indirect, and dynamic programming based approaches. In this work, we propose a process agnostic decomposition strategy to address Eq. (1) through the use of the Parametric Optimization and Control (PAROC) framework (Pistikopoulos et al., 2015). The proposed methodology comprises (i) developing an offline control policy that takes into account the different process dynamics stemming from the selection of the unit design and online economical decisions, (ii) deriving a scheduling policy based on the closed loop behavior of the system, and (iii) determining the design that minimizes the capital and operating costs for a given time period by utilizing the offline control and scheduling policies simultaneously.

2.3. Design-scheduling-control integration

The PAROC framework presents an *in-silico* environment to design offline model based receding horizon control and economical optimization policies (Pistikopoulos et al., 2015). In our previous works, we applied this framework on (i) the simultaneous process design and control problem where a design dependent control strategy is developed and embedded in a MIDO formulation to determine the control dependent optimal design (Diangelakis et al., 2017b), and (ii) the integrated scheduling and control problem where the dynamics of the offline control strategy is embedded in the schedule through a surrogate model formulation (Burnak et al., 2018b). Here, we propose a systematic approach to consider the design, scheduling, and control problems simultaneously by taking into account their interplay to yield cost effective and more reliable decisions.

The proposed methodology is based on developing explicit design dependent control and scheduling strategies to be directly implemented in a MIDO problem to determine the optimal design simultaneously with the control and scheduling decisions. In other words, we derive explicit functions for h and m in Eq. (1) that return the control and scheduling decisions, respectively.

In the proposed framework, the design, scheduling, and control decisions are based on a single dynamic high fidelity model that represents the essential characteristics of the system with sufficient accuracy. Using the high fidelity model, we derive each individual decision with an increasing order in their time scales, i.e. control, schedule, and design, respectively. Explicit strategies for both the control and the schedule include the decisions from their upper level problems as bounded parameters. Hence, the exact same control strategy is applicable under a range of operating set points from the schedule and different design options. Similarly, a single scheduling policy spans a range of different design realizations in real time operations. Furthermore, we develop a design dependent surrogate model formulation based on the closed loop dynamics of the system to account for the time scale difference between the scheduler and the controller. The derived offline strategies are nested in a MIDO formulation for the design optimization problem.

The following are the key steps of the PAROC framework tailored to address the integrated design, scheduling, and control problem, describing the derivation of (i) design dependent, schedule-aware controller, (ii) design dependent, control-aware schedule, and (iii) optimal design based on the offline control and scheduling policies, all summarized in Fig. 2. The interplay be-

tween the offline decision layers and the information flow in the overall MIDO formulation is illustrated in Fig. 2a. The derivation of the explicit MPC is explained schematically in Fig. 2b. Lastly, the derivation of the offline scheduler is summarized in Fig. 2c.

2.3.1. Design dependent and schedule-aware controller

We initialize the framework by mapping the upper level decision layers in an offline control strategy, described as follows. The development of the controller scheme, aware of the design and scheduling decisions, is summarized in Fig. 2b.

Step 1: High fidelity dynamic modeling. A rigorous and accurate representation of the system dynamics is postulated based on first principles, empirical correlations, and/or data-driven techniques. The resulting mathematical form is typically described by a set of differential algebraic equations (DAE), of which a generalized representation is given in Eq. (2).

$$\dot{x} = f(x(t), u(t), s(t), des, d(t), t)
y = g(x(t), u(t), s(t), des, d(t), t)$$
(2)

Step 2: Model approximation. The high fidelity model presented in Eq. (2) can be highly nonlinear for process systems, rendering it impractical to derive the explicit map of optimal control strategies. Therefore, we generate approximate models that accurately captures the dynamics of Eq. (2) based on subspace identification or model reduction techniques. In this study, we use the MATLAB System Identification ToolboxTM to approximate the high fidelity model, yielding the discrete time state space model given in Eq. (3).

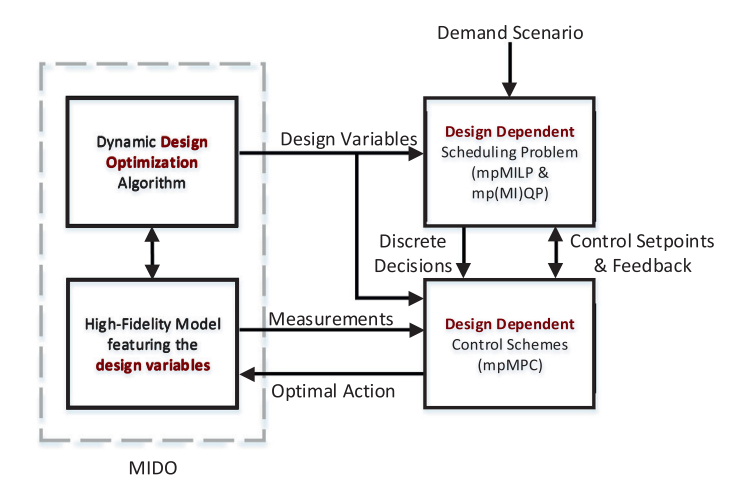
$$\begin{aligned} x_{t_c+1}^q &= A^q x_{t_c}^q + B^q u_{t_c} + C^q [d_{t_c}^T, s_{t_c}^T, des^T]^T \\ \hat{y}_{t_c} &= D^q x_{t_c}^q + E^q u_{t_c} + F^q [d_{t_c}^T, s_{t_c}^T, des^T]^T \end{aligned} \tag{3}$$

where $t_{\rm C}$ is the discrete time step of the controller, and \hat{y} is the output prediction. We also denote q as the index of the state space model, as multiple models can be used to identify different operating regions. Note that the scheduling and design decisions are treated as bounded parameters in the model. Also note that approximating a nonlinear process with a linear model creates a mismatch between the real output, y, and the predicted output, \hat{y} . Addressing the mismatch in designing the controller will be discussed in the next step.

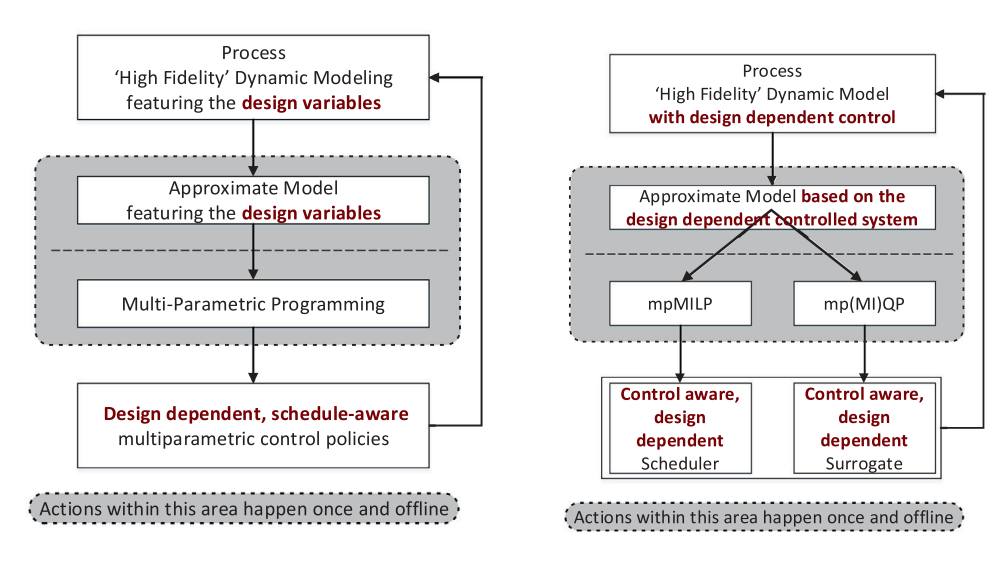
Developing accurate approximate representations of the high fidelity model is a pivotal step to generate reliable closed loop control strategies. Katz et al. (2018) investigated the effects of various model approximation techniques and introduces novel error metrics to evaluate the open and closed loop performances in the context of multiparametric programming. In this study, we employ these strategies to increase confidence in the approximate models developed. However these details are omitted here for brevity and to focus on the integration framework.

Step 3: Multiparametric model predictive control (mpMPC). The approximate model given by Eq. (3) is incorporated in a model predictive control (MPC) scheme that maintains closed-loop stability and set point tracking. The formulated MPC problem is converted into an mpMPC problem by treating the initial conditions, output set points, reference input trajectories, measured disturbances to the system, design and scheduling decisions as unknown but bounded parameters. Note that inclusion of the scheduling and control variables in the parametric space of the mpMPC problem results in a control strategy that is an explicit function of the decisions in the longer time scales. Therefore, regardless of the design and scheduling decisions, the exact same control strategy is applicable on the system. The generalized mpMPC problem formulation is presented in Eq. (4).

¹ Clearly, if a first principle high fidelity model is not available or derived, a grey box or data driven model can be used instead.



(a) Interplay between the process design, scheduling, and control layers.



(b) Explicit model predictive control as a (c) Explicit scheduling as a function function of design and scheduling actions. of design decisions and aware of closed The offline strategy is verified against the loop dynamics. The offline strategy is high fidelity model.

verified against the high fidelity model.

Fig. 2. The integration of process design, scheduling, and control decisions via multiparametric optimization.

$$\begin{split} u_{t_c}(\theta) &= \arg\min_{u_{t_c}} \quad \|x_{N_c}\|_P^2 + \sum_{t_c=1}^{N_c-1} \|x_{t_c}\|_Q^2 + \sum_{t_c=1}^{N_c-1} \|y_{t_c} - y_{t_c}^{SP}\|_{QR}^2 \\ &+ \sum_{t_c=0}^{M_c-1} \|u_{t_c} - u_{t_c}^{SP}\|_R^2 + \sum_{t_c=0}^{M_c-1} \|\Delta u_{t_c}\|_{R1}^2 \\ s.t. & x_{t_c+1} = Ax_{t_c} + Bu_{t_c} + C[d_{t_c}^T, s_{t_c}^T, des^T]^T \\ &\hat{y}_{t_c} = Dx_{t_c} + Eu_{t_c} + F[d_{t_c}^T, s_{t_c}^T, des^T]^T \\ &y_{t_c} = \hat{y}_{t_c} + e \\ &e = y_{t_c=0} - \hat{y}_{t_c=0} \\ &\underline{x} \leq x_{t_c} \leq \overline{x}, \quad \underline{y} \leq y_{t_c} \leq \overline{y} \\ &\underline{u} \leq u_{t_c} \leq \overline{u}, \quad \underline{\Delta u} \leq \Delta u_{t_c} \leq \overline{\Delta u} \end{split}$$

$$\theta = [x_{t_c=0}^T, u_{t_c=-1}^T, d_{t_c=0}^T, s_{t_c}^T, des^T]^T$$

$$\{y_{t_c}^{SP}, u_{t_c}^{SP}\} \subseteq s_{t_c}, \quad \forall t_c \in \{0, 1, \dots, N_c - 1\}$$
(4)

where θ is the set of bounded parameters, N_c is the output horizon, M_c is the control horizon, $\|\cdot\|_{\Psi}$ denotes weighted vector norm with a weight matrix Ψ , SP denotes set point, P, Q, QR, R, and R1 are the corresponding weight matrices. We also define an error term, e, to account for the mismatch between the actual system output and the predicted output at the time of measurement. Addition of the error to the model prediction carries over the mismatch through the entire output horizon.

Eq. (4) is reformulated into a multiparametric linearly constrained quadratic programming problem (mpQP) by using the YALMIP toolbox (Löfberg, 2004) and solved exactly by using the Parametric OPtimization (POP) Toolbox (Oberdieck et al., 2016).

The solution of the resulting problem yields explicit piecewise affine functions of the uncertain parameters for the control strategy, as presented in Eq. (5).

$$u_{t_c}(\theta) = K_n \theta + r_n, \quad \forall \theta \in CR_n$$

$$CR_n := \{ \theta \in \Theta \mid L_n \theta < b_n \}, \quad \forall n \in \{1, 2, \dots, NC\}$$
(5)

where CR_n is the active polyhedral partition of the feasible parameter space, NC is the number of critical regions, and Θ is a closed and bounded set.

Remark 1. The piecewise affine control strategy, u_{t_c} , is an explicit function of both the design and the scheduling decisions. Therefore, Eq. (5) is a single design dependent, schedule-aware mpMPC solution that is applicable under different operating conditions dictated by the upper level decision layers.

Step 4: Closed loop validation. The control strategy is developed based on an approximation of the real process dynamics, design decisions, and operating conditions. Therefore, validity of the controller is exhaustively tested *in-silico* against the actual process under numerous design alternatives and operating conditions dictated by the schedule. The control scheme is accepted if it maintains effective set-point tracking, fast adaptation to changes in the operating level, operational stability, while satisfying the process constraints. Otherwise, a new control strategy is developed by either tuning the weight matrices in the objective function of Eq. (4) or by deriving a new approximate model.

2.3.2. Design dependent and control-aware scheduler

Analogous to designing the control scheme, we aim to derive an offline map of the optimal scheduling decisions as a function of its complementing decisions. Burnak et al. (2018b) proposed a two level scheduling scheme with (i) an upper level problem that regulates the operation based on profitability and feasibility, and (ii) a lower level problem that translates the upper level decisions into the time steps of the control problem to bridge the time scale difference. In this work, we propose an extension to this approach by incorporating the design decisions explicitly into the map of scheduling actions. The steps to develop the offline receding horizon policies, and their implementation in the design optimization problem is summarized in Fig. 2c.

Step 1: High fidelity model with closed loop dynamics. The explicit expressions for the control strategy given by Eq. (5) is directly implemented in the high fidelity model (Eq. (2)). The resulting model describes the system with the closed loop dynamics.

Step 2: Model approximation. Inclusion of the explicit control law in the high fidelity model changes the dynamics of the system, and thus necessitates a new approximate model that represents the new dynamics. Therefore, we use the MATLAB System Identification ToolboxTM to approximate the output of the system for a given scheduling decision, such as the output set point and input reference trajectory. However, the time scale of the scheduling model is typically orders of magnitude greater than the time scale of the controller. This discrepancy is accounted for by resampling the scheduling model in finer time intervals that match the output horizon of the controller for the construction of a surrogate model in the next step.

Step 3: Multiparametric schedule and surrogate model. A common practice to determine optimal production schedule is to postulate an MILP problem that treats the processing times as fixed parameters. Subramanian et al. (2012) presents an excellent framework to transform this problem into an equivalent state space form that represents the system of interest. Kopanos and Pistikopoulos (2014) used multiparametric programming to derive the offline map of optimal schedule based on the transformed problem as an

explicit function of the initial conditions of the system and the demand rates. Burnak et al. (2018b) introduced an offline surrogate model formulation as a lower level scheduling decision to bridge the gap between the longer term scheduling actions and short term control strategies. In this study, we extend this approach by incorporating the design decision as a bounded uncertain parameter in both the scheduling and the surrogate model formulations.

A general representation of the longer term scheduling decisions is presented in Eq. (6).

$$s_{t_{s}}(\theta) = \arg\min_{s_{t_{s}}(\theta)} \sum_{t_{s}=1}^{N_{s}} \alpha^{T} x_{t_{s}} + \sum_{t_{s}=0}^{N_{s}-1} \beta^{T} s_{t_{s}}$$

$$s.t. \quad x_{t_{s}+1} = A x_{t_{s}} + B s_{t_{s}} + C d_{t_{s}}$$

$$s_{t_{s}} = [(y_{t_{s}}^{SP})^{T}, (u_{t_{s}}^{SP})^{T}]^{T}$$

$$\underline{x}_{t_{s}} \leq x_{t_{s}} \leq \overline{x}_{t_{s}}$$

$$\underline{s} Y_{t_{s}} \leq s_{t_{s}} \leq \overline{s} Y_{t_{s}}$$

$$\theta = [x_{t_{s}=0}^{T}, d_{t_{s}}^{T}]^{T}$$

$$\forall t_{s} \in \{0, 1, \dots, N_{s}\}$$

$$(6)$$

where the Greek letters α and β denote cost parameters, and $Y_{t_s} \subseteq s_{t_s}$ denotes the set of binary scheduling decisions that dictate the operating window based on the production regime. The state space matrices are derived at the previous step, and are different from the control model since they (i) represent the closed loop dynamics, and (ii) span a significantly greater time scale. Note that apart from the disruptive scheduling events, the design decision is included as a measured disturbance in d_{t_s} and treated as a bounded uncertain parameter in Eq. (6).

The schedule formulated in Eq. (6) is classified as a mp-MILP problem, which is solved exactly via the POP toolbox (Oberdieck et al., 2016). The solution is a piecewise affine expression that maps the optimal scheduling decisions offline as a function of the initial conditions of the system, any disruptive events in the future, and the design of the process.

We further need to address the gap between the scheduler and the controller stemming from the large time scale differences and the plant-model mismatch created by the approximation of the closed loop dynamics. Therefore, we formulate a surrogate model as an mpQP problem that readjusts the upper level scheduling decisions in the time steps of the control scheme, as presented in Eq. (7).

$$\underset{\tilde{s}_{t_{s}}(\theta)}{\operatorname{arg}} \quad \sum_{t_{sm}=0}^{N_{sm}} \|\tilde{s}_{t_{sm}} - s_{t_{s}=0}\|_{R}^{2}$$

$$s.t. \quad \tilde{x}_{t_{sm}+1} = A\tilde{x}_{t_{sm}} + B\tilde{s}_{t_{sm}} + Cd_{t_{sm}}$$

$$\tilde{s}_{t_{sm}} = \left[(\tilde{s}_{t_{sm}}^{SP})^{T}, (\tilde{u}_{t_{sm}}^{SP})^{T} \right]^{T}$$

$$\underline{x} \leq \tilde{x}_{t_{sm}} \leq \bar{x}$$

$$\underline{s}Y_{t_{sm}} \leq \tilde{s}_{t_{sm}} \leq \bar{s}Y_{t_{sm}}$$

$$\theta = \left[x_{t_{sm}=0}^{T}, d_{t_{sm}}^{T}, s_{t_{s}=0}^{T}, Y_{t_{sm}}^{T} \right]^{T}$$

$$\forall t_{sm} \in \{0, 1, \dots, N_{sm}\}$$
(7)

where the tilde symbol (\sim) denotes the scheduling variables readjusted by the surrogate model. Eq. (7) describes an mpQP problem that modifies the long term scheduling decisions from Eq. (6) in the time steps of the controller. The time steps of the surrogate model Δt_{sm} is selected such that one step spans the entire control horizon (i.e. $\Delta t_{sm} = \Delta t_c N_c$). Similarly, the output horizon of the surrogate model is set to be greater than the discretization step of the scheduler (i.e. $N_{sm} \geq \Delta t_s/\Delta t_{sm}$) to translate the scheduling decision at the first time step.

The solution to Eq. (7) maps the readjusted operating set points for the controller as a function of the longer term scheduling

decisions and design variables offline. During the online implementation, the set points passed to the controller are updated every Δt_{sm} time increments based on the states of the closed loop system and the upper level scheduling decisions by the explicit solution of Eq. (7).

Step 4: Closed loop validation. The hierarchical scheduling scheme is validated in tandem with the control strategy against the high fidelity model. The offline solutions of problems Eq. (6) and Eq. (7) are used simultaneously with Eq. (5) to govern the feasibility and profitability of the process described with Eq. (2). The offline strategies are tested against a range of design options and varying market scenarios. The scheduling schemes are accepted if they yield feasible and profitable closed loop profiles for the given range of design and market conditions uncertainties. Otherwise, the tuning parameter of the surrogate model is modified, or a new approximate model is derived for the closed loop dynamics.

2.3.3. Design optimization based on explicit scheduling and control

The offline maps for the optimal scheduling and control strategies draws explicit relations as a function of the design decisions. Therefore, incorporation of these functional forms for the operational decisions reduces the overall degrees of freedom of Problem 1 from the union of the design, scheduling, and control variables to the design variables only. Furthermore, direct inclusion of the design dependent operating strategies in the MIDO problem ensures the operability of the resulting design configuration for a range of process and market disturbances. For more details on embedding the multiparametric solution in a MIDO problem, the reader is referred to Diangelakis et al. (2017b).

Remark 2. Postulating all decision layers as optimization problems in the framework has practical benefits to be able to impose any physical limitations in each individual problem as hard or soft constraints. Such physical limitations can include safety considerations, thermodynamics, or operational policies. Implementation of these limitations is discussed and demonstrated in detail in the following examples.

Remark 3. The offline maps of optimal economical and operational decisions alleviate the computational burden of real-time optimization. During the online operation, we can simply determine the optimal actions *exactly* by a look-up table and affine function evaluations, instead of solving any optimization problems. On the other hand, determining the offline maps via multiparametric programming and solving the integrated MIDO problem can be computationally expensive. However, these steps of the framework are evaluated once and completely offline.

Remark 4. The aim of the proposed framework is *not* to determine the global minimum of Eq. (1). Due to pre-postulation of scheduling and control strategies in the design optimization problem, Eq. (1) in fact describes a lower bound on the reconstructed MIDO. However, the reference trajectories acquired by Eq. (1) may be unattainable by the scheduling and control schemes when they are not explicitly accounted for, resulting into suboptimal, even infeasible operations. The proposed framework guarantees the operability of the system by properly embedding the operational strategies.

Remark 5. The proposed framework is *not* geared towards speeding up the computational time to solve Eq. (1). Because the solution profile and objective value can be suboptimal to Eq. (1) in the proposed framework (see Remark 4), the MIDO algorithm may terminate faster compared to the monolithic solution. In other words, any observed speed up in computational time is due to the search for a suboptimal but operable design, rather than an artifact of the solution strategy.

3. Case studies

3.1. CSTR with three inputs and three outputs

This case study is adapted from Flores-Tlacuahuac and Grossmann (2006), a widely used problem for simultaneous scheduling and control studies. The CSTR is operated isothermally and is expected to deliver three products on a single production line, as presented in Fig. 3. In the figure, R_i denotes the ith reactant, P_j denotes the jth product, $Demand_{P_j}$ denotes the demand rate for product P_j , and V_{CSTR} denotes the volume of the CSTR. The reactor is allowed to produce a single product at a given time, and the product at the exit stream is required to satisfy a certain purity threshold to be stored in the inventory tanks. A time variant demand rate for all products is satisfied continuously from these tanks. Therefore, a feasible operation requires storing a nonzero amount of the products in the inventory tanks. The mathematical representation of the high fidelity model is given in Eqs. (A.1b)–(A.1h) in Appendix A.

The limitation on producing a single product at a given instance enforces the reactor to undergo transition regions between the productions of different products. The system dynamics during the transition regions are affected by the operation history and target operating points, which are ultimately dictated by the time variant demand rates and products stored in the inventories. These transitions should be accounted for while making economic operational decisions, as they cost raw materials and time. Therefore, incorporating the closed loop system dynamics in the scheduling decisions improves the economic performance of the reactor.

Considering this motivation, the problem statement is formulated as follows:

- Given: A high-fidelity model of the three product CSTR, unit inventory costs, a functional expression for the CSTR fixed cost, a scenario of product demands.
- (ii) Determine: Volume of the CSTR, production sequence, production rates, optimal reactant volumetric flow rates to achieve the target production rate and to reach the threshold purity.
- (iii) Objective: Minimize the sum of operating and capital costs.

The objective in the problem definition can be achieved by determining the reactor design, production schedule, and closed loop dynamics that minimize the wasted raw materials and processing time. Therefore, (i) the controller is expected to deliver optimal transitions between all operating points determined by the scheduler, (ii) the scheduling decisions have to minimize the operating costs while accounting for the closed loop dynamics, and (iii) the reactor must be large enough to remain feasible throughout the entire operation, while avoiding overdesign to minimize the capital costs.

We formulate the MIDO problem given in Eq. (A.1) to achieve the targeted goals. The following discussion breaks down the derivation and the solution strategy of the given multi-level MIDO problem.

High-fidelity dynamic model. The reaction network in the CSTR is given in Eq. (8).

$$2R_1 \rightarrow P_1$$

$$R_1 + R_2 \rightarrow P_2$$

$$R_1 + R_3 \rightarrow P_3$$
(8)

Eq. (8) shows that R_1 is required to produce all three products, and is the only raw material to produce P_1 . Based on the reaction stoichiometry, P_1 is expected to be generated as an impurity during the production of other products. Therefore, any control scheme needs to monitor the impurity level during the production periods

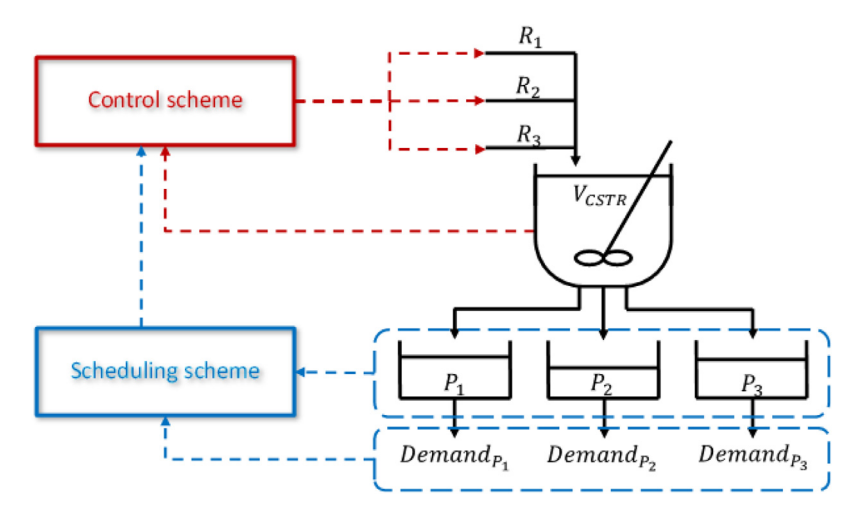


Fig. 3. Example 1 - CSTR flowsheet with the online implementation of the scheduling and control schemes.

to achieve high selectivity and satisfy the purity threshold. For further details regarding the governing equations and relevant system and cost parameters, the reader is referred to Burnak et al. (2018b)

Model approximation. This case study is used to illustrate using multiple approximate models to represent the dynamics of a single high fidelity model. The input space is partitioned into multiple mutually exclusive subspaces which are concatenated into a single state space representation. Note that using a single state space model model maintains the identical design dependence in every constituent subspace. MATLAB® System Identification ToolboxTM is used to derive the approximate model.

Determining the number of input partitions creates a tradeoff between the accuracy of the representation and computational complexity of solving the offline control problem. Rigorous open loop simulations of the high fidelity model suggest that two partitions for each degree of freedom is sufficient to capture the dynamics of the overall system. According to these simulations, the input space is set up as presented in Eq. (9).

$$u = [u_1, u_2, u_3, u_4]^T$$

$$u_1 = a_2, \ a_2 \in [0, 0.5)$$

$$u_2 = a_2, \ a_2 \in [0.5, 1]$$

$$u_3 = a_3, \ a_3 \in [0, 0.55)$$

$$u_4 = a_3, \ a_3 \in [0.55, 1]$$
(9)

where a_2 and a_3 are the volumetric fractions of R_2 and R_3 in the feed stream, respectively. Therefore, in the state space approximate model given in Eq. (3), x are the identified states, u are the volumetric fractions of the reactants with all respective partitions, d are the total volumetric flow rate and the reactor volume, and y are the product concentrations. The state space matrices and the step response profile of the model are given in Appendix B.

Design of the mpMPC. The control scheme is based on the standard MPC formulation given in Eq. (4) with two major additions: (i) Incorporation of mutually exclusive control decisions, (ii) Introduction of soft constraints to minimize the transition time in the control level.

In the model approximation step, we introduced mutually exclusive control decisions that account for different ranges of a given manipulated variable. A big-M formulation is employed to enforce the controller to select only one of the subspaces, as presented in Eq. (10).

$$\underline{u}z_i \le u_i \le \overline{u}z_i, i \in \{1, \dots, NP\}$$

$$\sum_{i=1}^{NP} z_i = 1$$
(10)

where u_i are continuous decision variables, z_i are binary decision variables, and NP denotes the number of partitions in the input space. Note that incorporating the binary variables results into an mpMIQP problem, for which the POP toolbox features an exact algorithm (Oberdieck et al., 2016).

The second addition to the control scheme aims to penalize the transition times between the production regimes. The soft constraints, presented in Eq. (11), features slack variables that have to take a nonzero value to satisfy the inequality.

$$-y^* + Pur_{min} \sum_{i \in Prod} y_i \le -\varepsilon + \mathcal{M}(1 - Y), \varepsilon \in [0, 1]$$
(11)

where y are the system outputs (i.e. molar concentrations), Pur_{\min} is the threshold purity level to initiate the production regime, ε are the slack variables, \mathcal{M} is the big-M parameter, Y is the binary switch parameter determined by the schedule, Prod is the set of products $\{P_1, P_2, P_3\}$, and "*" denotes the product of interest at a given time. Note that time subscript t is omitted for brevity. Eq. (11) forces the slack variables to be nonzero if the concentration of the product of interest is below the purity threshold. This purity constraint is enforced for all products, but is only activated or relaxed based on Y, determined by the schedule. Therefore, penalizing the slack variables along the output horizon entails minimizing the transition time. The additional penalty term used in the objective function of the control scheme is presented in Eq. (12).

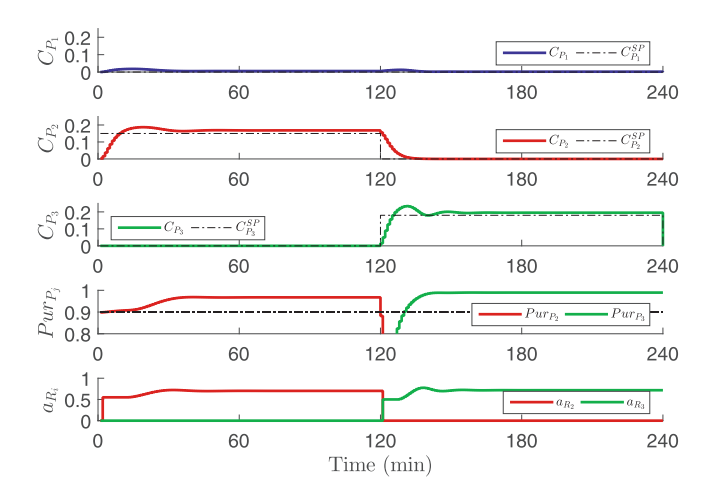
$$\sum_{t=1}^{M} \|\varepsilon_t\|_{P_1}^2 \tag{12}$$

where M is the control horizon, and P1 is a positive definite penalty matrix for the slack variables. Note that a linear penalty function will also derive the slack variables to zero, as they are defined as nonnegative variables. However, a quadratic penalty term is preferred to avoid any potential dual degenracies in the multiparametric problem.

The mpMPC is developed based on the standard form given in Eq. (4), with the addition of Eq. (12) in the objective function, and the inclusion of Eqs. (10) and (11) in the constraints. The control parameters are determined based on heuristic MPC tuning methods, and are provided in Table 2. It should be noted that the mpMPC scheme treats the two upper level decisions, i.e. total feed flow rate (schedule) and reactor volume (design) as bounded parameters. Therefore, the solution of the constructed mpMPC problem yields a unified explicit control strategy that accounts for a range of scheduling and design decisions that are specified in Table 2.

Table 2Tuning parameters for the mpMPC of the CSTR for Example 1.

mpMPC Design Parameters	Value
N _c	6
M_c	2
QR	$\begin{bmatrix} 10^2 & 0 & 0 \\ 0 & 10 & 0 \\ 0 & 0 & 10 \end{bmatrix}$
R1	50
P1	90
Pur _{min}	0.9
у	$[0, 0, 0]^T$
<u>u</u>	$[0, 0.5, 0, 0.55]^T$
<u>d</u>	$[0, 0.4]^T$
у <u>u</u> <u>d</u> <u>ў</u> п	$[1, 1, 1]^T$
\overline{u}	$[0.5, 1, 0.55, 1]^T$
$\frac{d}{d}$	$[500, 1.0]^T$



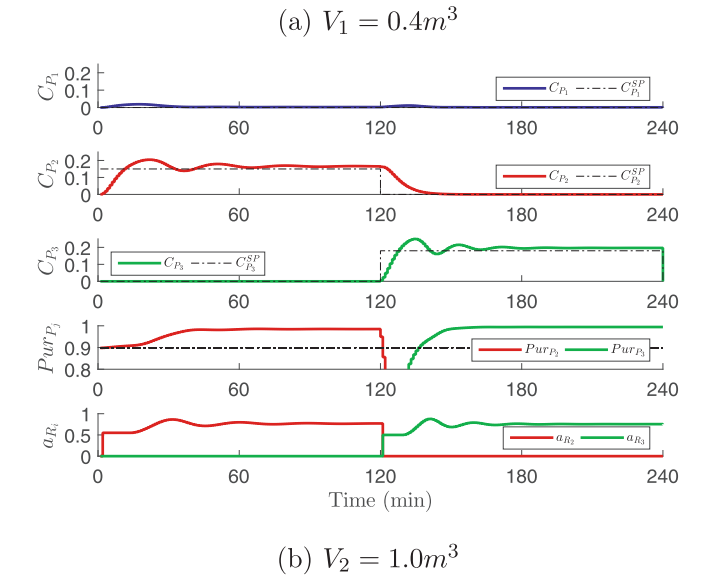


Fig. 4. Example 1 - Step change in set points in two reactors with different volumes.

Closed loop validation. The developed mpMPC is validated against the high-fidelity model, under a range of scheduling decisions and design options. Fig. 4 presents 4 h closed loop simulations for two reactor volumes ($V_1 = 0.4 \, m^3$, $V_2 = 1.0 \, m^3$). The process undergoes a step change from P_2 to P_3 after 2 h of operation to test the validity of the control scheme under different schedul-

ing decisions and design configurations. Note that all operations are governed by a single explicit control law that is a function of the design and scheduling decisions.

The closed loop simulations presented in Fig. 4 shows that the developed control scheme is suitable for a range of scheduling and design options. The control scheme (i) achieves effective set point tracking for all three products simultaneously, (ii) minimizes transition time by prioritizing the purity satisfaction, (iii) recognizes the dynamics introduced by different scheduling decisions and design configurations, and (iv) maintains the operation within the inherent/imposed bounds of the system.

High-fidelity model with the mpMPC embedded. The explicit control law is integrated to the original high fidelity model. The integrated model yields the closed loop dynamics of the system that is required to formulate the scheduling problem.

Model approximation. Two approximate models are derived with the discretization time steps of the scheduler (1 h) and the controller (1 min), respectively. For this particular example, the approximate model for the scheduler is derived based on a simplified first principle mole balance as presented in Eq. (13) instead of an input-output based system identification. The mole balance expressions yield linear expressions that are directly implemented in a scheduling problem in the form of an mpMILP (Burnak et al., 2018b).

$$\frac{dW_j}{dt} = F_j - DR_j \tag{13}$$

where W_j is the inventory level, F_j is the product molar flow rate at the exit of the reactor, and DR_j is the demand rate of product P_j , respectively.

Three surrogate models are identified for three distinct products via the MATLAB System Identification Toolbox. The surrogate models take the total volumetric flow rate and reactor volume as inputs and determines the product concentration set point and reference reactant composition at the feed based on the closed loop behavior. The state space matrices and the step and impulse responses of the surrogate models are presented in Appendix B.

Design of the scheduler. The objective of the schedule is to minimize the inventory costs while satisfying continuous demand rate forecast within the scheduling horizon. Therefore, the objective function to be minimized is formulated as presented in Eq. (14).

$$\sum_{i=1}^{N_s} \sum_{t=1}^{N_s} \alpha_j W_{j,t} \tag{14}$$

where N_s is the scheduling horizon, α_j is the storage unit cost, and $W_{j,t}$ is the inventory level of P_j at discretized time step t. This objective function is subjected to the governing dynamic approximate model given in Eq. (13), discretized as presented in Eq. (15).

$$W_{i,t+1} = W_{i,t} + \Delta t F_{i,t} - \Delta t D R_{i,t}, \quad \forall j, \quad \forall t \in \{1, \dots, N_s - 1\}$$
 (15)

The reactor is allowed to produce one product at a given time instance. Therefore, product assignment constraints are employed to enforce the system to select only one product at a time, as presented in Eq. (16).

$$\sum_{j=1}^{\infty} y_{j,t} = 1$$

$$\underline{F}y_{j,t} \le F_{j,t} \le \overline{F}y_{j,t}$$
(16)

Capacity constraints are used to impose the physical limitations of the storage tanks, as presented in Eq. (17).

$$\underline{W} \le W_{i,t} \le \overline{W} \tag{17}$$

Table 3System parameters of the scheduling problem for Example 1.

System parameters	Value
N _s	3
α (\$/h.mol)	$[1.0, 1.5, 1.8]^T$
$\Delta t(min)$	60
\overline{F}	$[50, 50, 50]^T$
\overline{W}	$[50, 50, 50]^T$
\overline{D}	$[60, 60, 60]^T$
<u>F</u>	$[0, 0, 0]^T$
<u>W</u>	$[0, 0, 0]^T$
<u>D</u>	$[0, 0, 0]^T$

The initial conditions and the demand rate forecast are defined as uncertain and bounded parameters as presented in Eq. (18).

$$\theta = [W_{j,t=0}, DR_{j,t}]$$

$$\theta < \theta < \overline{\theta}$$
(18)

Therefore, the overall scheduling problem is constructed to minimize Eq. (14), subjected to Eqs. (15)–(18). The parameters of the scheduling problem are provided in Table 3.

Design of the surrogate model. The time scale gap between the scheduler and the controller is addressed by a quadratic objective function that minimizes the L^2 norm between the volumetric flow rate determined by the schedule and the transformed decision that is passed to the controller, as presented in Eq. (19). An additional term is included for the slack variables that take place in the purity governing soft constraints.

$$\sum_{t=0}^{M_{sm}} \|Q_{total,t} - \tilde{Q}_{total,t}\|_{R'}^2 + \sum_{t=1}^{N_{sm}} \|\varepsilon_t'\|_{P1'}^2$$
(19)

where $\tilde{Q}_{total,t}$ is the scheduling decision, and is defined in Eq. (20).

$$\tilde{Q}_{total,t} = \frac{\sum_{j} F_{j,t}}{C_{P^*,t=0}} \tag{20}$$

The objective function constructed in Eq. (19) is subjected to the approximate closed loop dynamic models given in Appendix B, box constraints on the inputs, outputs, and the parameters (Eq. (21)), as well as the purity soft constraints (Eq. (11) discretized in the time steps of the surrogate model).

$$\underline{u} \leq u_t := [Q_{total,t}, C_{j,t}^{SP}, \varepsilon_t'] \leq \overline{u}$$

$$\underline{y} \leq y_t := [C_{j,t}] \leq \overline{y}$$

$$\underline{d} \leq d := [\tilde{Q}_{total,t}, des] \leq \overline{d}$$
(21)

Three mpQP problems are constructed for three products. The surrogate model parameters are tuned to improve the closed loop performance, and are provided in Table 4.

Closed loop validation of the integrated scheduling and control scheme. The controller, surrogate model, and the scheduler are operated simultaneously on the high fidelity model under a range of design options and product demand variations. Fig. 5 showcases the closed loop profiles for 12 h at the lower bound $(V_1 = 0.4 \, m^3)$ and the upper bound $(V_2 = 1.0 \, m^3)$ of the design range. Note that the same design dependent offline strategies are used in two reactors. The demand profiles for the products are randomly regenerated every hour, and the scheduling decisions are updated in a rolling horizon manner. The closed-loop simulations validate that the integrated scheduling and control scheme (i) maintains low inventory levels in the storage tanks, (ii) reactively adapts to changes in the demand profile, (iii) is applicable for a range of different design options. A sample of the offline scheduling and control decisions is demonstrated in Table 5, where a snapshot of the online

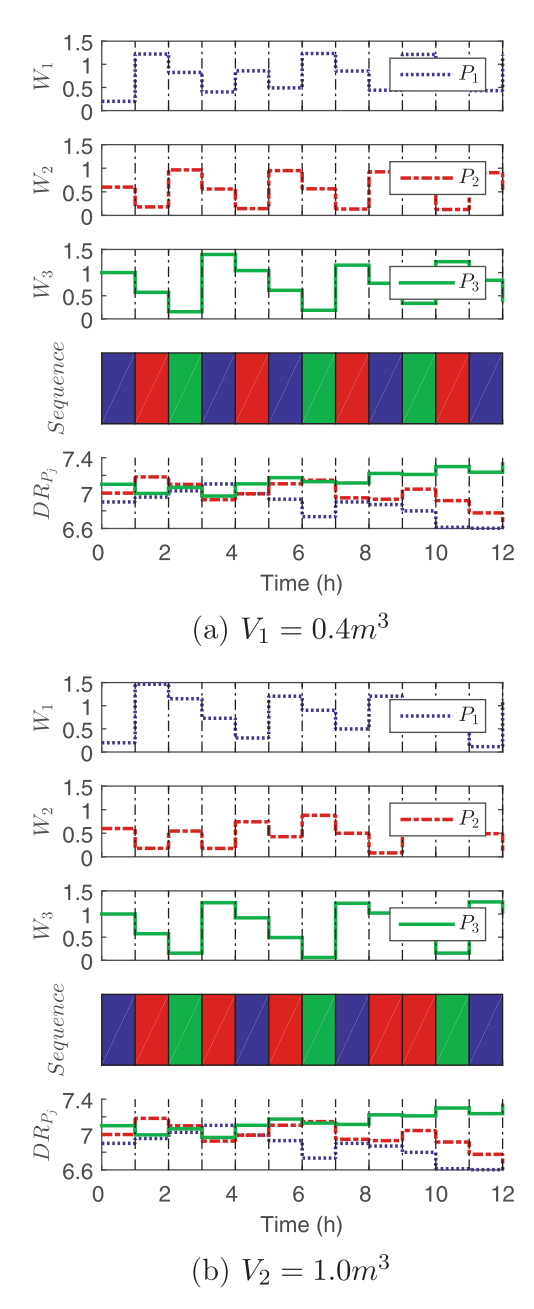


Fig. 5. Example 1 - Closed-loop validation of the integrated scheduling and control scheme in two reactors with different volumes.

operation of the large CSTR at $t=5\,\mathrm{h}$ is tabulated. Such explicit expressions are available for the range of design decisions, and will be used for design optimization described as follows.

Design optimization. The validated offline scheduling and control strategies are embedded in the overall MIDO problem given in Eq. (1) in the gPROMS environment. The capital investmentment for the reactor is determined by Eq. (22) (Towler and Sinnott, 2013).

$$C_e = a + bV^n \tag{22}$$

where C_e is the annualized reactor cost, and a, b, n are cost parameters given in Appendix C, along with the cost escalation indexes for year 2018. The minimum total annual cost is found as \$330k/yr at $V = 0.69 \, m^3$. Note that the scheduling and control strategies yield feasible operation for the optimal reactor volume as a result of their design dependence. Therefore, treating the design, scheduling, and control problems simultaneously ensures the operability

Table 4System parameters for the surrogate model for Example 1.

System parameters	Model 1	Model 2	Model 3
N _{sm}	10	10	10
M_{sm}	1	1	1
Δt_{sm} (min)	6	6	6
R'	10 ³	$\begin{bmatrix} 10^{-4} & 0 \\ 0 & 10^{-1} \end{bmatrix}$	$\begin{bmatrix} 10^{-4} & 0 \\ 0 & 10^{-1} \end{bmatrix}$
P1'	10 ⁴	10 ⁶	108
\overline{u}	$[500, 1, 1, 1, 1, 1, 1]^T$	$[500, 1, 1, 1, 1, 1, 1]^T$	$[500, 1, 1, 1, 1, 1, 1]^T$
$\frac{\overline{u}}{\overline{d}}$	$[1, 1, 1]^T$	$[1, 1, 1]^T$	$[1, 1, 1]^T$
\overline{d}	$[500, 1.0]^T$	$[500, 1.0]^T$	$[500, 1.0]^T$
<u>u</u>	$[0, 0, 0, 0, 0, 0, 0]^T$	$[0, 0, 0, 0, 0, 0, 0]^T$	$[0, 0, 0, 0, 0, 0, 0]^T$
	$[0, 0, 0]^T$	$[0, 0, 0]^T$	$[0, 0, 0]^T$
<u>y</u> <u>d</u>	$[0, 0.4]^T$	$[0, 0.4]^T$	$[0, 0.4]^T$

Table 5 Example 1 - An illustration of the offline map of receding horizon policies at t=5 h for the large CSTR ($V_2=1.0\,m^3$). Observe that the volume of the reactor has a direct impact on the control action for this particular instance.

Decision variable	Affine expression
$F_{3,t=0}$ $F_{2,t=1h}$ $F_{1,t=2h}$ $Q_{total,t=0}$	$= -16.7W_3 + DR_{3,t=0} + DR_{3,t=1h} + DR_{3,t=2h}$ $= -16.7W_2 + DR_{2,t=0} + DR_{2,t=1h} + DR_{2,t=2h}$ $= -16.7W_1 + DR_{1,t=0} + DR_{1,t=1h} + DR_{1,t=2h}$ $= 500$
$CP_{2,t=0}^{SP}$ a_1 a_2	$ = 0.91(CP_{1,t=0} - 0.003) - 0.007(CP_{2,t=0} - 0.14) - 0.12 $ $ = 0.45 - 6 \times 10^{-3}V $ $ = 0.55 + 6 \times 10^{-3}V $

of the system, as the MIDO problem comprises the exact closed loop strategies that will be used online during the operation.

3.2. Two CSTRs operating in parallel

This case study presents an extension of the single CSTR example discussed in Section 3.1 to two CSTRs operating in parallel. The exact same control strategy and the surrogate model formulations are employed because the open loop dynamics of the system remains unchanged. The cooperative operation of the two CSTRs is maintained by a centralized scheduler that allocates the production tasks on the reactors based on their volumes and their production regimes at a given time.

Design of the scheduler. The governing approximate model given in Eq. (15) is generalized to represent multiple CSTRs operating in parallel, as presented in Eq. (23).

$$Wj, t+1 = Wj, t + \sum_{p=1}^{N_{CSTR}} \Delta t F_{j,t,p} - \Delta t DR_{j,t} \quad \forall j, \forall t \in \{1, \dots, N_s - 1\}$$
(23)

where the number of the reactors, N_{CSTR} , equals 2 by the problem definition. The product assignment constraints are also generalized as presented in Eq. (24).

$$\sum_{j=1} y_{j,t,p} = 1$$

$$\underline{F}y_{j,t,p} \le F_{j,t,p} \le \overline{F}y_{j,t,p}$$
(24)

Closed loop validation. The generalized offline scheduling scheme is validated against the high fidelity model of the two reactor system. Fig. 6 showcases a scenario with one small reactor $(V_1 = 0.4 \, m^3)$ and one larger reactor $(V_2 = 1.0 \, m^3 3)$ operated in parallel. The integrated scheduling and control scheme is able to drive the inventory level of the most costly product, W_{P_3} , close to zero by assigning it to the larger reactor. The large reactor is capable of satisfying the demand on P_3 standalone, and the small reactor has

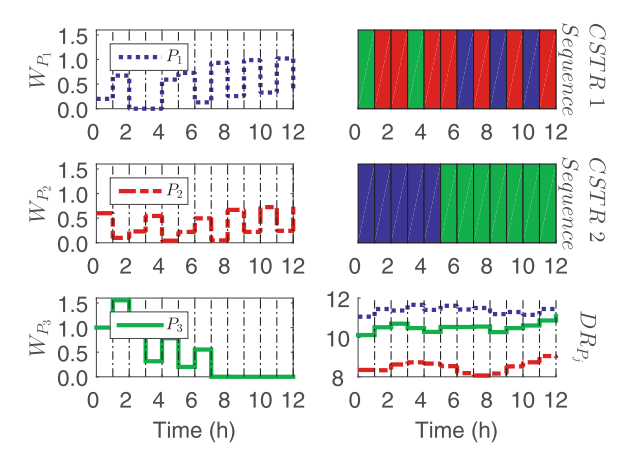


Fig. 6. Example 2 - Closed loop validation of the generalized scheduling scheme in two reactors operating in parallel. The volumes of the reactors are $V_1 = 0.4 \, m^3$ and $V_2 = 1.0 \, m^3$, respectively.

a faster transition rate because of the lower retention time. Therefore recognizing the closed loop dynamics and the capacity of the reactors, the integrated schedule assigns the costly product, P_3 , to the large reactor, and alternates the production between P_1 and P_2 in the small reactor.

Design optimization. The offline maps of scheduling and control are embedded in the overall MIDO problem in the gPROMS environment. The reactor configuration with volumes $V_1 = 0.44 \, m^3$ and $V_2 = 0.92 \, m^3$ minimizes the total annual cost accounting for the capital and operating costs. Note that one large reactor and one small reactor is selected to deliver (i) uninterrupted production of one of the products depending on their unit storage prices and demand rates throughout the horizon, and (ii) fast transitions for alternating production of the remaining products, respectively.

3.3. Residential combined heat and power (CHP) unit

This case study presents an application of a combined heat and power generation system (CHP) on a residential scale. In our previous work (Diangelakis et al., 2017b), we developed design dependent explicit controllers to simultaneously optimize the design and control decisions in a MIDO formulation. In this study, we extend this approach by taking into account the external factors that affect the desired level of operation, i.e. the fluctuations in the heat and power demand rates, and changing market prices for the electricity and fuel. We consider a residential district with 10 units, all of which are supplied hot water for heating purposes and electricity from a single CHP unit. The hot water can be stored in a buffer tank if the produced heat content exceeds the demand rate. Additional electricity can be supplied from the central grid if the

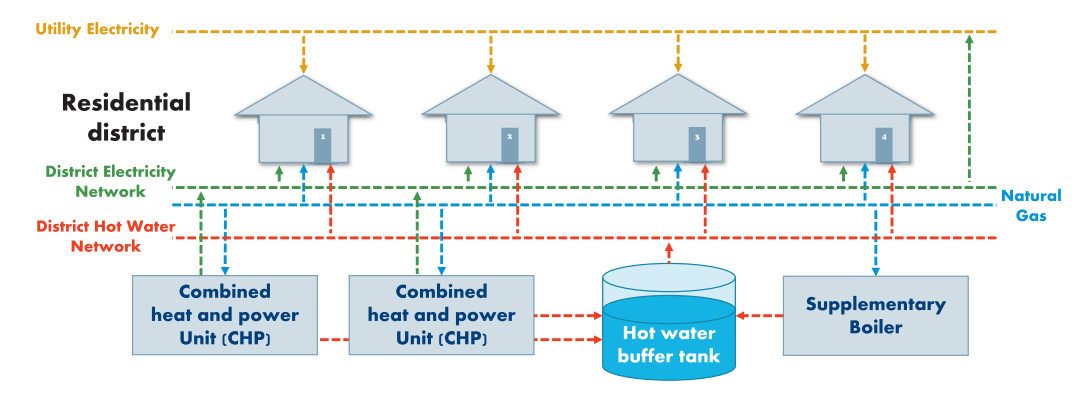


Fig. 7. Example 3 - A generalized flowsheet of the CHP system.

CHP unit falls short, and a supplementary boiler is assumed to be available at all times to provide more heat content. Excess electricity produced from the CHP unit can be sold to the central grid for revenue, and excess hot water can be disposed of at an expense. Note that the rapidly changing electricity prices in day time and night time has a significant economic impact on the operation of a CHP unit. For instance, it may be more profitable to operate the CHP unit at a higher capacity during the day time because of the increased cost of electricity purchase, and at a lower capacity at the night time when the cost decreases. Therefore, determining the most cost effective operation can be achieved by taking into account the fluctuation in the prices, demands rates, as well as the dynamics of the CHP units. A generalized flowsheet of the CHP system with two parallel CHP units is presented in Fig. 7. However in this section, we focus on a system with a single CHP system supplying the heat and power to the residential units. Parallel operation of multiple units will be discussed in the subsequent example.

The problem statement of the problem is given as follows:

- (i) Given: A high-fidelity model of the CHP, a demand scenario for electricity and heat consumption, investment cost of the CHP unit as a function of its size, market prices of fuel and purchasing/selling electricity.
- (ii) Determine: Internal combustion engine (ICE) size of the CHP, a schedule for the transactions with the grid and fuel purchases, operating level of the CHP.
- (iii) Objective: Minimize the sum of operating and capital costs.

The size of the ICE directly affects the process time of the system, and thus the responsiveness of the CHP to fluctuations in the demand rates and market prices. ICEs smaller in size have lower transition time, hence they can deliver fast responses to changes in the operating set points. On the other hand, larger ICEs can supply more power and heat to the residential units when the demand rates are high. The trade-off between the responsiveness and the capacity of the CHP is addressed by integrating a design dependent scheduler and controller in the design optimization problem.

High-fidelity dynamic model. There are two main components taken into account in the CHP model, (i) a natural gas powered ICE to produce electrical power, and (ii) a cooling system that recovers the excess heat content of the ICE. We also include the dynamics of the throttle valve that manipulates the inlet air mass flow rate, and the intake manifold that distributes the air into the ICE cylinders. For the detailed mathematical model, the reader is referred to Diangelakis et al. (2014).

Model approximation. The original high fidelity model is a DAE system with 364 algebraic and 15 differential relations in the continuous domain. In our previous studies, the complexity of the overall system is addressed by decomposition into two approximate models, namely a power production subsystem and a heat recovery subsystem (Diangelakis et al., 2016; 2017b). The former

operating mode gives the relation between the throttle valve opening and the power output of the CHP, while the latter is used to estimate the water temperature at the outlet as a function of the power output and the water flow rate into the heat recovery system. Eq. (25) presents the identified state-space model for the power production subsystem.

$$x_{t+1} = 0.9799x_t + 0.0006u_t + 6.516V$$

$$y_t = 7.839x_t$$
(25)

where x_t is the identified state, u_t is the throttle valve opening, V is the volume of the ICE, y_t is the electrical power generated by the CHP.

The heat recovery subsystem is an explicit function of the output of the power production subsystem and is given in Eq. (26).

$$x_{t+1} = \begin{bmatrix} 0.997 & 0.103 & -0.003 \\ -0.002 & 0.940 & 0.116 \\ -0.058 & -0.056 & 0.179 \end{bmatrix} x_t + \begin{bmatrix} -0.008 & 0.001 \\ 0.280 & -0.033 \\ -1.280 & 0.146 \end{bmatrix} u_t$$

$$y_t = \begin{bmatrix} -529.9 & -2.827 & 0.252 \end{bmatrix} x_t$$
(26)

where x_t is the set of identified states, u_t are the power generation level and water flow rate, respectively, and y_t is the temperature of the hot water at the outlet. The discretization time steps of the models presented in Eqs. (25) and (26) are both 0.1 s.

Design of the mpMPC. The two subsystems derived in the previous step are operated by a decentralized control policy, which comprises interlinked control strategies for each subsystem. We define two operational modes for the decentralized control policy defined as follows.

- Electricity driven mode (Mode 1): The operating level of the CHP, i.e. the power set point, is determined based on the power demand. Therefore, the throttle valve opening is manipulated primarily to satisfy the demand on electricity. The operating level projected by the electricity generation subsystem is treated as a measured disturbance by the heat recovery subsystem, hence the produced heat is a function of the power output of the CHP. The heat production level of a standalone CHP unit can be insufficient to satisfy the heat demand at a given time, requiring the use of the supplementary boiler. It is also possible that the produced heat content exceeds the heat demand, in which case the hot water is stored in a buffer tank.
- Heat production driven mode (Mode 2): The operating level of the CHP is determined based on the heat demand. Tracking a water temperature set point at 70°C, heat recovery subsystem (i) determines an operating level set point to ensure sufficient heat production by the power production subsystem, and (ii) manipulates the cooling water flow rate to recover enough heat

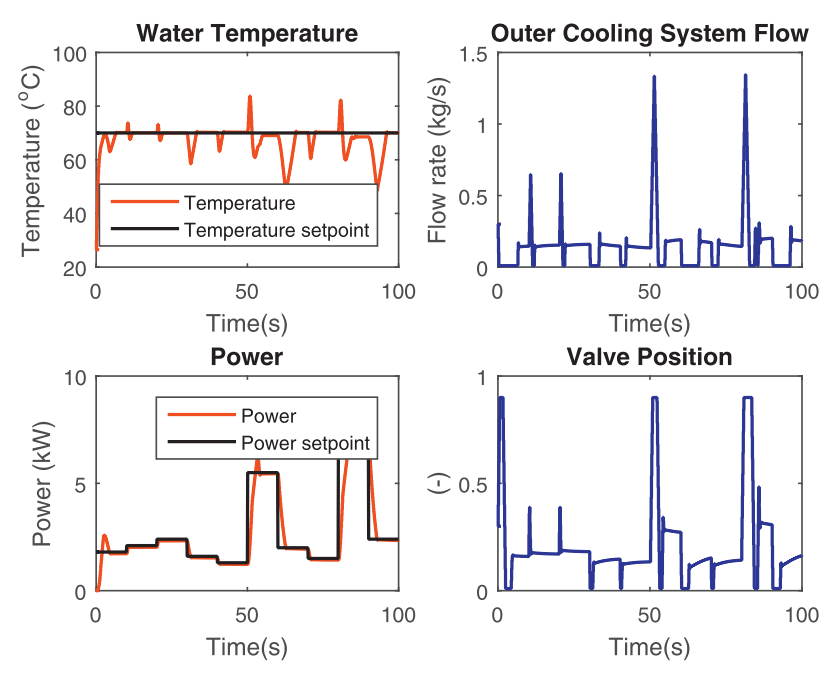


Fig. 8. Example 3 - Closed loop simulation of a CHP unit with V = 1500cc, operated with mode 1.

to satisfy the demand. Analogous to mode 1, the power production level may not match the electricity demand. In case of insufficient power, additional electricity is purchased from the central grid, and excess electricity is sold back to the grid for revenue.

The reader is referred to Diangelakis et al. (2016), Diangelakis et al. (2017b) and Diangelakis and Pistikopoulos (2017) for more details on the operating modes and a quantified evaluation of the decentralized control policy.

Note that changing the operating modes creates an offset between the new set point and the current output of the system. This offset has economical consequences on the operation and dictates the quantity of electricity purchases/sales, usage of the buffer tank and the supplementary boiler. These economical aspects are addressed and mitigated in the following steps.

Closed loop validation. The design dependent decentralized control policy is validated against the high fidelity model under a range of different design and scheduling decisions. Fig. 8 shows a closed loop simulation of a CHP with $V=1500{\rm cc}$ operated with mode 1 only. The power set point is subject to random changes throughout the operation.

Similarly, closed loop simulation on a larger CHP (V = 5000cc) is demonstrated in Fig. 9. Note that due to operating mode 2, the power set point is subject to changes dictated by the heat recovery subsystem.

High fidelity model with the mpMPC embedded. The explicit form of the decentralized control policy is implemented in the original high fidelity model.

Model approximation. The closed loop high fidelity model is used to develop an approximate model for the scheduler via the MATLAB System Identification Toolbox. The identified model establishes a relation between the power production and heat storage levels, and the change in the power production set point, as presented in Eq. (27).

$$\begin{bmatrix} E_{t+1} \\ B_{t+1} \end{bmatrix} = \begin{bmatrix} 0.999 & 0 \\ 37.9 & 0.955 \end{bmatrix} \begin{bmatrix} E_t \\ B_t \end{bmatrix} \begin{bmatrix} 99.5 & 0 & 0 \\ 0 & 11.2 & -11.2 \end{bmatrix} \begin{bmatrix} R_t \\ Q_t \\ D_t \end{bmatrix} + \begin{bmatrix} 0 \\ -11.2 \end{bmatrix} \zeta_t^h$$
(27)

where E_t is the energy production level, B_t is the heat storage level, R_t is the change in the power production set point, Q_t is the additional heat supplied from the boiler, D_t is the disposed heat, ζ_t^h is the heat demand, and the time step of the model is 10 s. We also use an overall energy balance for the relation between the power production, power demand, and electricity purchases from the central grid, presented in Eq. (28).

$$P_t + E_t = \zeta_t^p + W_t \tag{28}$$

where P_t is the electricity purchase, ζ_t^p is the power demand, and W_t is the excess electricity sold back to the grid.

Design of the scheduler. The objective of the schedule is to minimize the operating costs, including energy production, energy purchases and sales, and inventory costs, as given in Eq. (29).

$$\sum_{t=1}^{N_s} \beta E_t + \psi_t P_t - \nu_t W_t + \xi_t Q_t + \omega_t D_t + \gamma B_t$$
 (29)

where the Greek letters denote the corresponding cost parameters. Note that the CHP unit is assumed to be operational throughout the scheduling horizon. Hence, on/off switching costs are excluded in the objective function. This assumption will be relaxed in Section 3.4 where we discuss a parallel operation of multiple CHP units. The objective function is subject to the approximate CHP model derived in Eqs. (27) and (28), as well as the lower and upper bounds on the optimization variables.

The power production capacity of the CHP unit is a function of the ICE size (i.e. $\overline{E} = \overline{E}(V)$). The schedule treats this design variable as a bounded parameter along with the initial conditions of the system, power and heat demands, unit cost of purchasing fuel and power, and unit revenue of selling power, as listed in Eq. (30).

$$\theta = [V, E_t, B_t, \zeta_t^h \zeta_t^p, \beta_t, \psi_t, \nu_t, \xi_t, \omega_t, \gamma_t]$$
(30)

Design of the surrogate model. Eqs. (27) and (28) are resampled in the time steps of the controller, and substituted in the surrogate model formulation presented in Eq. 7. The resampled state space matrices are given in Appendix B.

Closed-loop validation. The integrated scheduling and control scheme is validated against an extensive set of design options and demand profiles. Fig. 10 shows a snapshot of a closed loop simulation of a CHP unit with a volume V = 5000cc. Note that the

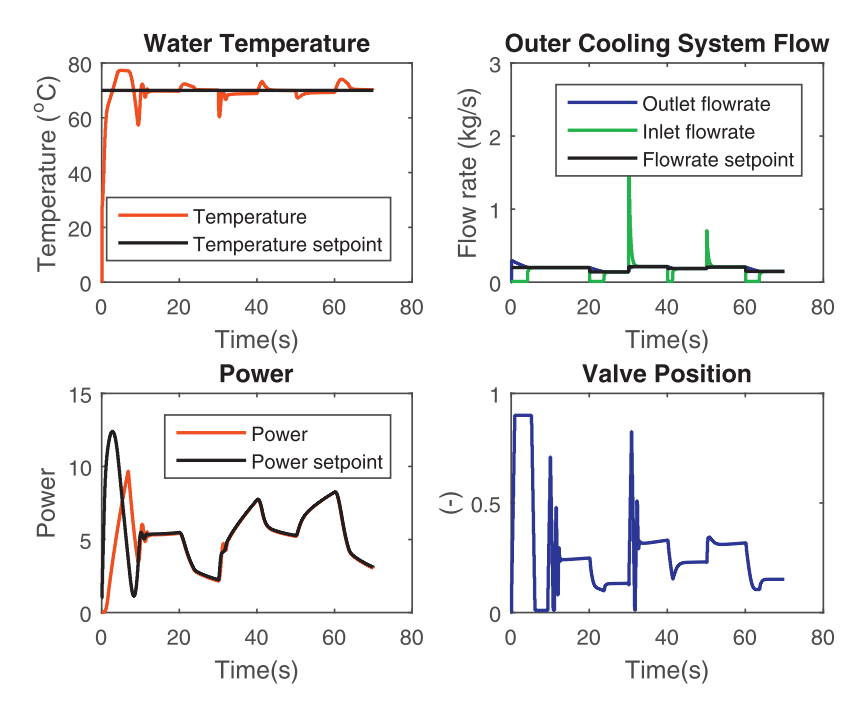


Fig. 9. Example 3 - Closed loop simulation of a CHP unit with V = 5000cc, operated with mode 2.

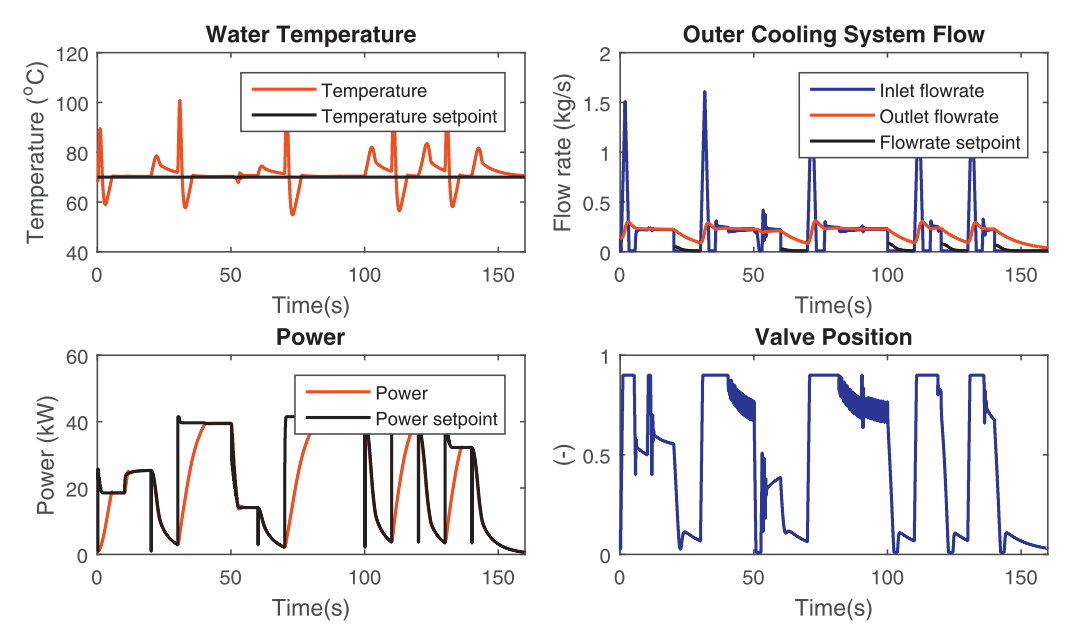


Fig. 10. Example 3 - Closed-loop validation of the integrated scheduling and control scheme on a CHP with V = 5000cc.

power set point throughout the operation is determined by the offline schedule, and translated into the time steps of the controller by the surrogate model.

Design optimization. We formulate a MIDO problem in the gPROMS environment using the high fidelity model, the explicit design dependent relations for the scheduler, surrogate model, and the controller. The capital investment cost is assumed to be a linear function of V, and is given in Appendix C. A CHP unit with an ICE volume of V=1710 cc yields the scheduling and control strategies that minimizes the total annualized cost that includes the capital and operating costs.

3.4. Two CHPs operating in parallel

The single CHP case study presented in Section 3.3 is extended to include two CHP units operating in parallel. We

generalize the scheduling formulation to account for multiple CHP units, and showcase the proposed algorithm on a system with two units. We also include the dynamics stemming from switching on/off the units, and their impact on the operational optimization.

Design of the scheduler. Evidently, multiple CHP units have a greater capacity to supply heat and power compared to a single unit. However, the total production rate of multiple units can exceed the demand rates significantly even when they are operated at their lowest capacities. In other words, operating one CHP unit standalone can be more cost effective than operating two CHPs simultaneously at low demand rates. Therefore, we include the start-up and shut-down dynamics in the schedule to account for the trade-off between switching on/off the operation and maintaining the operating status of a unit.

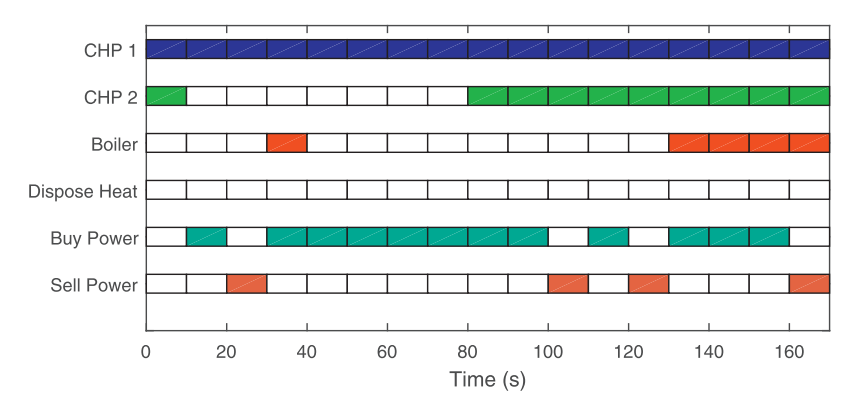


Fig. 11. Example 4 - Closed loop simulation of the generalized scheduling scheme in two CHP units operating in parallel. The volumes of the ICE are $V_1 = 1500$ cc and $V_2 = 4500$ cc, respectively.

The cost of switching on/off is described by Eq. (31).

$$\sum_{i=1}^{N_{CHP}} \sum_{t=1}^{N_{s}} \phi_{i} S_{i,t} + \pi_{i} F_{i,t}$$
(31)

where N_{CHP} is the number of CHP units, $S_{i,t}$ and $F_{i,t}$ are binary variables that indicate the start-up and shut-down status, and ϕ_i and π_i are their unit costs, respectively. The impact of the switching status variables is incorporated in the schedule by introducing lifting-state variables, $\tilde{S}_{i,t,n}$ and $\tilde{F}_{i,t,n}$, as presented in Eq. (32).

$$\tilde{S}_{i,t+1,n} = \tilde{S}_{i,t,n-1}, \quad \tilde{S}_{i,t,n=0} = S_{i,t}
\tilde{F}_{i,t+1,n} = \tilde{F}_{i,t,n-1}, \quad \tilde{F}_{i,t,n=0} = F_{i,t}$$
(32)

The state lifting-variables determine the operating status of the CHP units as described in Eq. (33).

$$S_{i,t} - F_{i,t} = X_{i,t} - X_{i,t-1}$$

$$X_{i,t} \ge \sum_{n=0}^{\delta_i^{up}} \tilde{S}_{i,t,n} \tag{33}$$

$$1 - X_{i,t} \ge \sum_{n=0}^{\delta_i^{dn}} \tilde{F}_{i,t,n}$$

where $X_{i,t}$ is a binary variable that indicate the operating status, δ_i^{up} and δ_i^{dn} are the start-up and shut-down times of the ith CHP unit. The interested reader is referred to Subramanian et al. (2012) for more details on scheduling with lifting-state variables, and to Kopanos and Pistikopoulos (2014) for an application of reactive scheduling using lifting-state variables on a CHP system.

The cost function given in Eq. (29) is generalized to encapsulate the operating cost of multiple CHP units, as presented in Eq. (34).

$$\sum_{i=1}^{N_{CHP}} \sum_{t=1}^{N_s} \beta E_{i,t} + \sum_{t=1}^{N_s} \psi_t P_t - \nu_t W_t + \xi_t Q_t + \omega_t D_t + \gamma B_t$$
 (34)

The objective function of the schedule comprises the operating and purchasing costs described by Eq. (34) and the switching costs given in Eq. (33).

Closed loop validation. The developed scheduling strategy is implemented on the high fidelity model and operated in tandem with the offline controller. Fig. 11 shows a snapshot of the scheduling level decisions of an operation with two CHP units with ICE volumes $V_1 = 1500 \, \text{cc}$ and $V_2 = 4500 \, \text{cc}$, under a rapidly escalating demand profile given in Fig. 12. The following are some observations and remarks on the closed loop performance of the developed scheduling and control strategies.

• The small CHP is operated standalone at low demand rates.

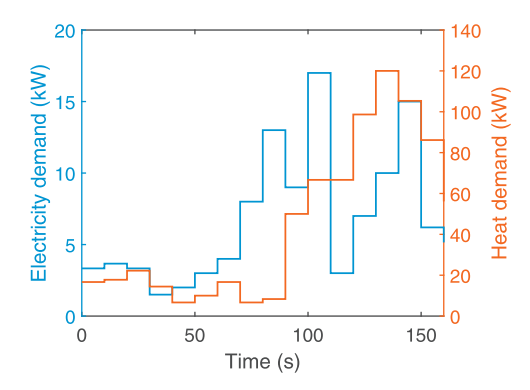


Fig. 12. Example 4 - Snapshot of the electricity and heat demand profiles. Note the steep increase in demand in short notice.

- The large CHP is operated when either of the demand rates are high.
- Due to the time loss during the start-up of the large CHP, grid electricity is used to supplement the deficit.
- The recovered heat content is not wasted by disposal.
- In both CHP units, set point tracking is achieved via the same design-dependent control strategy, which is developed and discussed in Section 3.3. The closed loop profiles of water temperature, power output, cooling water flow rate, and valve position are omitted here fore brevity.

Design optimization. The MIDO problem is formulated by embedding the offline scheduling and control schemes in the high fidelity model in the gPROMS environment. A CHP system with ICE volumes of $V_1=2050{\rm cc}$ and $V_2=2700{\rm cc}$ yields the most cost effective scheduling and control strategies, minimizing both the capital and operating costs. Note that one small CHP unit is selected to be operated continuously even at low demand rates, and one larger CHP unit to be operational under higher demand rates, a similar outcome of the case study presented in Section 3.2.

4. Conclusions

In this study, we introduced a novel, process agnostic framework to integrate the design, scheduling, and control problems based on a single high fidelity model. Using multiparametric programming, we derived offline piecewise strategies for (i) a control scheme as a function of the design and scheduling decisions, (ii) a scheduling scheme as a function of design, and aware of the closed-loop dynamics through a surrogate model formulation. The offline maps of strategies allowed for a direct implementation in a MIDO formulation for design optimization. The proposed

framework was able to determine the process design that guarantees the operability of the system under a range of bounded process and market uncertainties by simultaneously considering the optimal scheduling and control strategies used in closed-loop implementation.

Postulating all layers of decisions as optimization problems has specific benefits to tailor each individual problem based on the needs of the system of interest. This advantage was illustrated by using soft constraints to satisfy product purity in the CSTR examples, and by using a decentralized control structure in the CHP examples. Note that the framework was applied on both problems without appealing to further modifications.

The computational complexities of the proposed framework arise in solving the multiparametric programming problems and the integrated MIDO problem. The former scales exponentially with the number of optimization variables and constraints, which is commensurate with the degrees of freedom of the control problem, number of scheduling decisions, and prediction horizon of the operating strategies. However, the parametric solution provides piecewise affine functions that are directly incorporated into the MIDO problem. Handling these piecewise affine functions in the integrated MIDO problem is less significant compared to the computational burden associated with the inherent nonlinearities of the open loop design optimization problem.

The major bottleneck of the proposed framework is employing approximate models in the control and scheduling levels. Although the confidence on the models were increased by using well-established and previously proposed error metrics (Katz et al., 2018), the approximation creates a mismatch between the real process dynamics and the decision making optimization problems. Future work will focus on incorporating robust counterparts of the scheduling and control problems to account for the mismatch. However, robust multiparametric receding horizon policies result in an explosion in the number of critical regions in the parametric solution space. This explosion should be handled by theoretical developments in multiparametric programming to explore larger critical regions in volume, and using a partial solution with the critical regions that occupy the significant portion of the parametric solution space.

Acknowledgments

Financial support from the National Science Foundation (Grant No. 1705423), Texas A&M Energy Institute, Shell Oil Company, Rapid Advancement in Process Intensification Deployment (RAPID) Institute, and Clean Energy Smart Manufacturing Innovation Institute (CESMII) is greatly acknowledged.

Appendix A. Complete MIDO formulation of integrated design, scheduling, and control problem for Example 1

The mathematical representation of the integrated design, scheduling, and control problem for Example 1 is given by Eq. (A.1), in the form of an MIDO formulation.

$$\min_{u,s,des} \overbrace{a + bV^n}^{\text{Fixed cost}} + \overbrace{\int_0^{\tau} \sum_{i \in P} \alpha_i(t) W_i(t) dt}^{\text{Operating cost}} \tag{A.1a}$$

s.t.
$$\frac{dC_i}{dt} = \frac{Q_i C_i^f - Q_{total} C_i}{V} + \sum_{i \in I} s_{i,j} \mathcal{R}_j, \quad i \in (R \cup P)$$
 (A.1b)

$$\mathcal{R}_{j} = k_{j} \prod_{i \in \mathcal{P}_{i}} C_{i}^{\nu_{j}}, \quad j \in J$$
(A.1c)

$$Q_{total} = \sum_{i \in R} Q_i \tag{A.1d}$$

$$\frac{dW_i}{dt} = \begin{cases} Q_{total}C_i - DR_i, & \text{if } Pur_i \ge 0.90 \\ -DR_i, & \text{if } Pur_i < 0.90 \end{cases}, i \in P$$
 (A.1e)

$$Pur_i = \frac{C_i}{\sum_{i \in P} C_i} \tag{A.1f}$$

$$a_i = \frac{Q_i}{Q_{total}}, i \in R \tag{A.1g}$$

$$des := [V] \tag{A.1h}$$

$$\begin{split} F_{i,t_s}(\theta_s) &= \arg\min_{u_{t_s}} \quad \sum_{i} \sum_{t_s} \alpha_{i,t_s} W_{i,t_s} \\ s.t. \quad W_{i,t_s+1} &= W_{i,t_s} + \Delta t_s F_{i,t_s} - \Delta t_s D R_{i,t_s} \\ &\underline{F}(V) y_{i,t_s} \leq F_{i,t_s} \leq \overline{F}(V) y_{i,t_s} \\ &\sum y_{i,t} = 1 \\ &\underline{W} \leq F_{i,t_s} \leq \overline{W} \\ \theta_s &= [V, W_{i,t_s=0}, D R_{i,t_s}] \\ t_s &\in \{0, \Delta t_s, \dots, N_s \Delta t_s\} \end{split} \tag{A.1i}$$

$$\begin{split} s &= \arg\min \quad \sum_{t_{sm}} \|Q_{total,t_{sm}} - \widetilde{Q}_{total,t_{sm}}\|_{R'}^2 + \sum_{t_{sm}} \|\varepsilon_{t_{sm}}'\|_{P1'}^2 \\ s.t. \quad x_{t_{sm}+1} &= A_{sm}x_{t_{sm}} + B_{sm}s_{t_{sm}} + C_{sm}des \\ \widetilde{Q}_{total,t_{sm}} &= \frac{\sum_{i} F_{i,t_{sm}}}{C_{t_{sm}=0}^*} \\ \theta_{sm} &= [C_{t_{sm}=0}^T, F_{i,t_{sm}}^T, des^T]^T \\ \underline{s} &\leq s_{t_{sm}} \leq \overline{s} \\ \underline{C} &\leq C_{t_{sm}} \leq \overline{C} \\ t_{sm} &\in \{0, \Delta t_{sm}, \dots, N_{sm}\Delta t_{sm}\} \end{split} \tag{A.1j}$$

$$s := [Q_{total,t_{sm}}(\theta_{sm}), C_{i,t_{sm}}^{SP}(\theta_{sm})]$$
(A.1k)

$$u = \arg \min_{a_{i,t_c}, \varepsilon_{t_c}, z_p} \sum_{t_c=1}^{N_c-1} \|C_{i,t_c} - C_{i,t_c}^{SP}\|_{QR}^2 + \sum_{t_c=0}^{M_c-1} \|\Delta u_{t_c}\|_{R1}^2 + \sum_{t=1}^{N_c} \|\varepsilon_{t_c}\|_{P1}^2$$

$$s.t. \quad x_{t_c+1} = A_c x_{t_c} + B_c u_{t_c} + C_c [d_{t_c}^T, s_{t_c}^T, des^T]^T$$

$$\hat{C}_{i,t_c} = D_c x_{t_c} + E_c u_{t_c} + F_c [d_{t_c}^T, s_{t_c}^T, des^T]^T$$

$$C_{i,t_c} = \hat{C}_{i,t_c} + e$$

$$e = C_{i,t_c=0} - \hat{C}_{i,t_c=0}$$

$$\underline{u}z_p \leq u_{t_c} \leq \overline{u}z_p$$

$$\sum_{p \in NP} z_p = 1$$

$$- C_{t_c}^* + Pur_{min} \sum_{i} C_{i,t_c=0} \leq -\varepsilon_{t_c} + \mathcal{M}(1 - Y_{t_c}^*)$$

$$\underline{x} \leq x_{t_c} \leq \overline{x}, \quad \underline{C}_i \leq C_{i,t_c} \leq \overline{C}_i$$

$$\underline{u} \leq u_{t_c} \leq \overline{u}, \quad \underline{\Delta u} \leq \Delta u_{t_c} \leq \overline{\Delta u}$$

$$\theta = [x_{t_c=0}^T, u_{t_c=-1}^T, d_{t_c=0}^T, s_{t_c}^T, des^T]^T$$

$$\forall t_c \in \{0, 1, \dots, N_c - 1\}, z_p \in \{0, 1\}, i \in P \quad (A.11)$$

Table A1Parameters of the high-fidelity CSTR model.

Reaction rate constants	Value	Reactant concentration at the feed	Value	Unit cost	Value
k_1	0.1	$C_{R_1}^f$	1.0	α_1	1.0
k_2	0.9	$C_{R_2}^{f}$	0.8	α_2	1.5
k_3	1.5	$C_{R_3}^f$	1.0	α_3	1.8

$$u := [a_{i,t_c}(\theta_c), \varepsilon_{t_c}(\theta_c), z_p(\theta_c)]$$
(A.1m)

The objective function, given by Eq. (A.1a), takes into account the annualized investment cost as a function of the reactor volume, and the operating cost as a function of the stored product in the inventory. Eqs. (A.1b)–(A.1h) are the dynamic high fidelity model of the multiproduct CSTR. More specifically, Eq. (A.1b) is the mass balance for the set of reactants (R) and products (P), Eq. (A.1c) is the rate expression for all reactions (I), Eq. (A.1d) is the volume balance at the exit of the reactor (mixture density is assumed to be constant), Eq. (A.1e) is the dynamics of the inventory levels in the storage tanks, Eq. (A.1f) is the purity of product $I \in P$, and Eq. (A.1g) defines the volumetric fraction of the reactants at the inlet. The The scheduling decisions are governed by Eqs. (A.1i) and (A.1j) to determine the operating region, and the closed loop control is regulated by Table A.6. The parameters of the high-fidelity CSTR model are provided in Table A.6.

$$D = \begin{bmatrix} 2.73 \cdot 10^{-2} & -7.48 & 3.03 & 2.02 \cdot 10^{-2} & -8.16 \cdot 10^{-2} & 6.13 \cdot 10^{-2} & 4.94 \cdot 10^{-1} \\ 5.82 & 4.97 & 9.08 \cdot 10^{-1} & -3.16 \cdot 10^{-1} & -3.06 \cdot 10^{-1} & 1.61 \cdot 10^{-2} & 4.02 \cdot 10^{-2} \\ -7.05 & 7.30 & 1.34 & 2.82 \cdot 10^{-1} & -4.33 \cdot 10^{-1} & 5.46 \cdot 10^{-2} & 4.80 \cdot 10^{-2} \end{bmatrix}$$
(B.1f)

Observe that the scheduling and control decisions are postulated as lower level optimization problems, nested in an MIDO problem. Due to the implicit nature of the lower level optimization problems, Eq. (A.1) is a challenging class of problem. Multiparametric programming allows for an offline map of solutions of the lower level decisions that can be implemented exactly in the upper level optimization problem.

Appendix B. Approximate models with their step responses

Here, we provide the approximate model that represents the open loop dynamics of the CSTR used in Example 1. The closed form of the state space model is given in Eqs. (B.1a) and (B.1b), and the corresponding matrices are provided in Eqs. (B.1c)–(B.1f).

$$x_{t_c+1} = Ax_{t_c} + B \begin{bmatrix} u_{1,t_c} \\ u_{2,t_c} \\ u_{3,t_c} \\ u_{4,t_c} \end{bmatrix} + C \begin{bmatrix} Q_{total,t_c} \\ V \end{bmatrix}$$
(B.1a)

$$\hat{C}_{i,t_c} = Dx_{t_c}, \quad i \in P \tag{B.1b}$$

$$B = \begin{bmatrix} 2.35 \cdot 10^{-3} & -1.47 \cdot 10^{-3} & -1.82 \cdot 10^{-3} & 3.36 \cdot 10^{-3} \\ 1.46 \cdot 10^{-3} & -1.36 \cdot 10^{-3} & 3.38 \cdot 10^{-3} & -1.76 \cdot 10^{-3} \\ 2.69 \cdot 10^{-3} & -5.12 \cdot 10^{-3} & 7.85 \cdot 10^{-3} & -7.13 \cdot 10^{-3} \\ -7.75 \cdot 10^{-3} & 5.44 \cdot 10^{-3} & 1.62 \cdot 10^{-2} & 6.43 \cdot 10^{-3} \\ -3.56 \cdot 10^{-3} & 2.36 \cdot 10^{-3} & 5.31 \cdot 10^{-3} & 1.37 \cdot 10^{-3} \\ 1.51 \cdot 10^{-2} & -1.36 \cdot 10^{-2} & -3.41 \cdot 10^{-2} & -5.63 \cdot 10^{-3} \\ -1.28 \cdot 10^{-2} & -4.08 \cdot 10^{-3} & -1.10 \cdot 10^{-2} & -3.00 \cdot 10^{-3} \end{bmatrix}$$

$$(B.1d)$$

$$C = \begin{bmatrix} -5.37 \cdot 10^{-6} & 9.54 \cdot 10^{-7} \\ 5.32 \cdot 10^{-6} & -1.05 \cdot 10^{-6} \\ -5.07 \cdot 10^{-5} & 9.44 \cdot 10^{-6} \\ -2.50 \cdot 10^{-5} & 4.15 \cdot 10^{-6} \\ -8.96 \cdot 10^{-7} & 6.44 \cdot 10^{-8} \\ 4.86 \cdot 10^{-5} & -8.22 \cdot 10^{-6} \\ 5.89 \cdot 10^{-5} & -1.07 \cdot 10^{-5} \end{bmatrix}$$
(B.1e)

where x_{t_c} is the vector of identified states. The step responses of the product concentrations with respect to the system inputs, scheduling, and design variables are presented in Fig. B.1.

Similarly, the approximate models that represent the closed loop dynamics are given in Eqs. (B.2)–(B.4). Note that the discretization time of the models are identical at 15 min.

Surrogate model 1.

$$x_{t_{sm}+1} = \begin{bmatrix} 0.004 & -0.001 & 0.002 \\ -0.031 & -0.010 & 0.045 \\ -0.118 & -0.026 & 0.118 \end{bmatrix} x_{t_{sm}}$$

$$+ \begin{bmatrix} -7.2 \\ -4.7 \\ -3.1 \end{bmatrix} 10^{-4} Q_{total,t_{sm}} + \begin{bmatrix} 1.7 \\ 1.4 \\ 2.1 \end{bmatrix} 10^{-3} V$$

$$\hat{C}_{i,t_{sm}} = \begin{bmatrix} 0.340 & -0.037 & 0.066 \\ 0.072 & -0.040 & 0.031 \\ 0.048 & -0.042 & 0.041 \end{bmatrix} x_{t_{sm}}, \quad i \in P$$

$$(B.2)$$

$$A = \begin{bmatrix} 9.67 \cdot 10^{-1} & 8.00 \cdot 10^{-4} & -2.30 \cdot 10^{-3} & -9.15 \cdot 10^{-2} & -2.31 \cdot 10^{-3} & -2.00 \cdot 10^{-3} & 5.12 \cdot 10^{-4} \\ 2.10 \cdot 10^{-3} & 9.65 \cdot 10^{-1} & -1.19 \cdot 10^{-2} & 8.36 \cdot 10^{-3} & -7.93 \cdot 10^{-2} & 4.75 \cdot 10^{-3} & -3.89 \cdot 10^{-2} \\ 7.49 \cdot 10^{-3} & -7.53 \cdot 10^{-3} & 8.61 \cdot 10^{-1} & 2.14 \cdot 10^{-2} & -1.06 \cdot 10^{-1} & 3.47 \cdot 10^{-2} & 1.36 \cdot 10^{-1} \\ 6.56 \cdot 10^{-2} & 1.72 \cdot 10^{-2} & 1.27 \cdot 10^{-2} & 9.54 \cdot 10^{-1} & 1.04 \cdot 10^{-2} & 2.27 \cdot 10^{-1} & -3.09 \cdot 10^{-2} \\ 1.87 \cdot 10^{-2} & 1.79 \cdot 10^{-2} & 2.19 \cdot 10^{-2} & 3.88 \cdot 10^{-4} & 9.85 \cdot 10^{-1} & 8.79 \cdot 10^{-2} & -3.98 \cdot 10^{-2} \\ -1.44 \cdot 10^{-1} & -1.51 \cdot 10^{-2} & -1.93 \cdot 10^{-2} & -7.41 \cdot 10^{-2} & -1.38 \cdot 10^{-2} & 5.65 \cdot 10^{-1} & 1.48 \cdot 10^{-2} \\ 1.49 \cdot 10^{-2} & 1.13 \cdot 10^{-1} & -3.65 \cdot 10^{-3} & -3.18 \cdot 10^{-3} & -8.20 \cdot 10^{-3} & 5.79 \cdot 10^{-3} & 6.95 \cdot 10^{-1} \end{bmatrix}$$

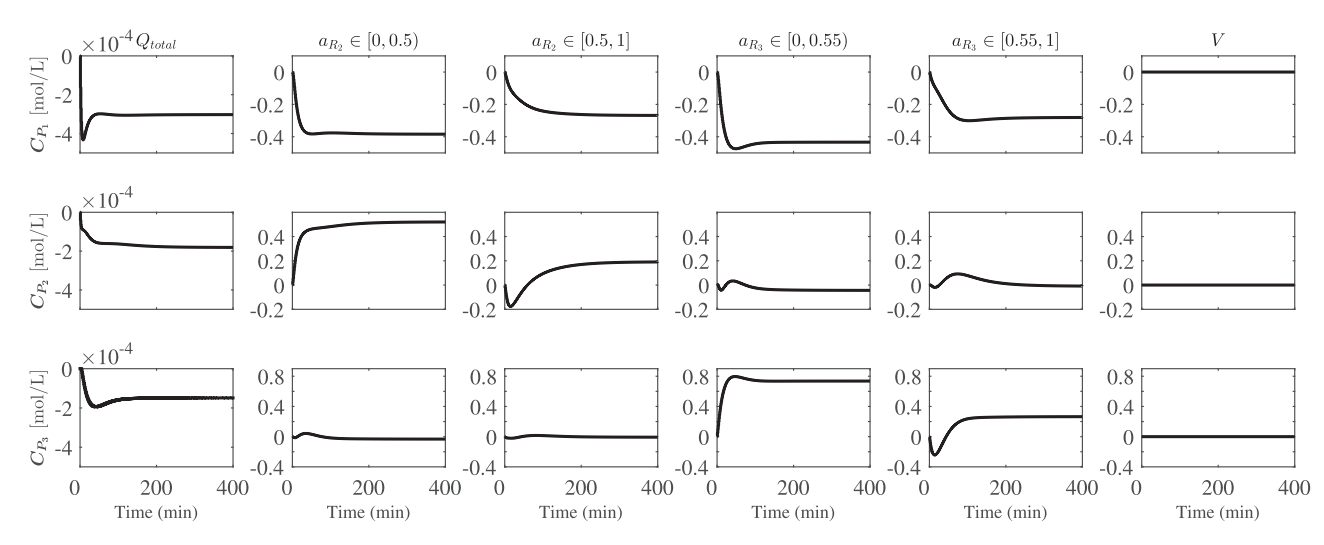


Fig. B.1. Step response of the identified approximate model with respect to the system inputs, as well as scheduling and design variables (Qtotal and V, respectively).

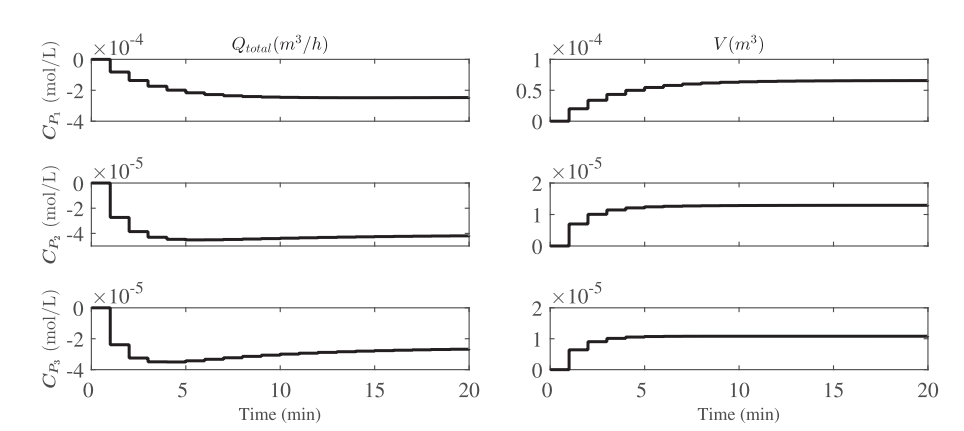


Fig. B.2. Step response of Surrogate Model 1 with respect to the scheduling (Q_{total}) and design decisions (V).

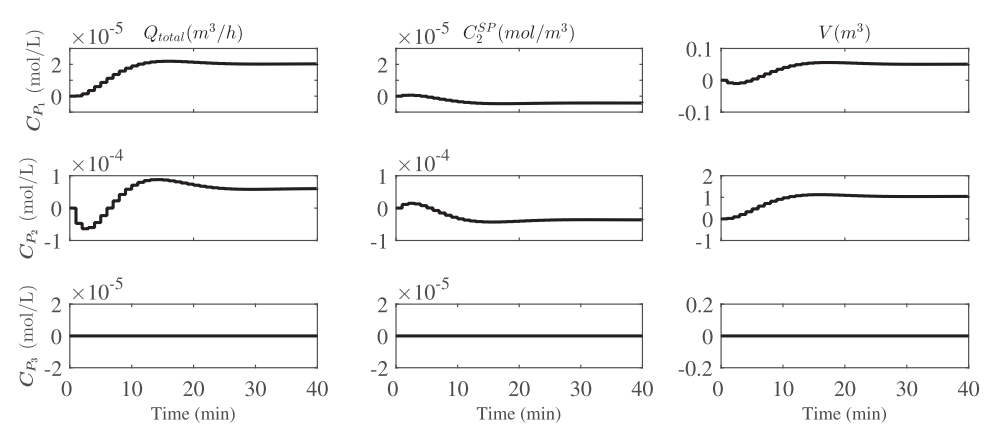


Fig. B.3. Step response of Surrogate Model 2 with respect to the scheduling (C_2^{SP}, Q_{total}) and design decisions (V).

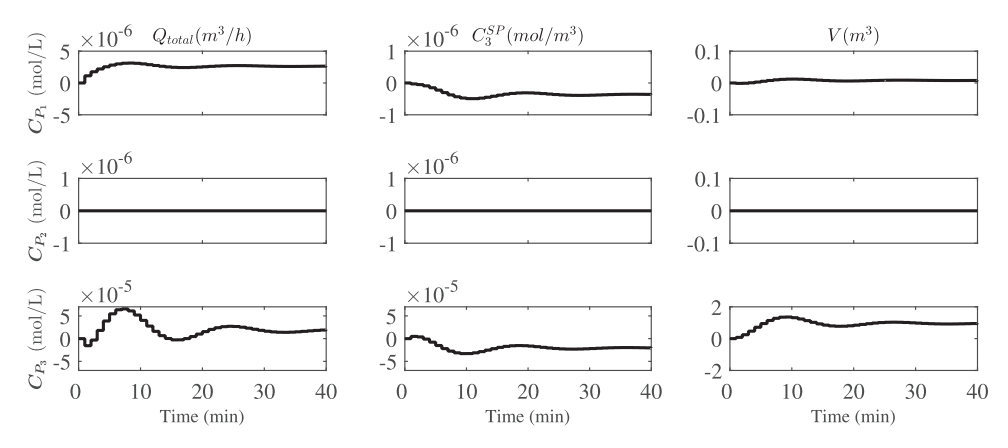


Fig. B.4. Step response of Surrogate Model 3 with respect to the scheduling (C_3^{SP}, Q_{total}) and design decisions (V).

Surrogate model 2.

$$\begin{split} x_{t_{sm}+1} &= \begin{bmatrix} 0.045 & 0.027 & -0.012 \\ 0.089 & -0.022 & -0.035 \\ 0.027 & 0.021 & -0.092 \end{bmatrix} x_{t_{sm}} \\ &+ \begin{bmatrix} 2.4 \cdot 10^{-4} & 0.130 \\ 9.0 \cdot 10^{-5} & -0.749 \\ 2.9 \cdot 10^{-6} & -0.716 \end{bmatrix} \begin{bmatrix} Q_{total,t_{sm}} \\ C_{P_2,t_{sm}}^{SP} \end{bmatrix} + \begin{bmatrix} -3.8 \\ 0.2 \\ 3.5 \end{bmatrix} 10^{-5}V \\ \hat{C}_{i,t_{sm}} &= \begin{bmatrix} 0.105 & -0.038 & -0.018 \\ 0.738 & -1.005 & -0.381 \\ 0 & 0 & 0 \end{bmatrix} x_{t_{sm}}, \quad i \in P \end{split}$$

$$(B.3)$$

Surrogate model 3.

$$\begin{split} x_{t_{sm}+1} &= \begin{bmatrix} -0.011 & -0.012 & -0.016 \\ -0.067 & 0.112 & 0.117 \\ 0.134 & -0.148 & 0.220 \end{bmatrix} x_{t_{sm}} \\ &+ \begin{bmatrix} 2.5 \cdot 10^{-4} & 0.171 \\ 9.8 \cdot 10^{-5} & -0.620 \\ -5.5 \cdot 10^{-5} & 0.192 \end{bmatrix} \begin{bmatrix} Q_{total,t_{sm}} \\ C_{P_3,t_{sm}}^{SP} \end{bmatrix} + \begin{bmatrix} -2.5 \\ 0.2 \\ -1.0 \end{bmatrix} 10^{-5}V \\ \hat{C}_{i,t_{sm}} &= \begin{bmatrix} 0.014 & -0.008 & 0.004 \\ 0 & 0 & 0 \\ 0.516 & -1.081 & 0.477 \end{bmatrix} x_{t_{sm}}, \quad i \in P \end{split}$$

$$(B.4)$$

where x_{t_c} is the vector of identified states. The step responses of the surrogate models are provided in Figs. B.2–B.4.

The closed form of the approximate model used in the surrogate model formulation for the CHP system (Examples 3 and 4) is given in Eq. (B.5).

$$\begin{bmatrix} E_{t_{sm}+1} \\ B_{t_{sm}+1} \end{bmatrix} = \begin{bmatrix} 1.0000 & 0 \\ 0.3880 & 0.9995 \end{bmatrix} = \begin{bmatrix} E_{t_{sm}} \\ B_{t_{sm}} \end{bmatrix} + \begin{bmatrix} 0.9954 & 0 & 0 \\ -19.2613 & 0.1143 & -0.1143 \end{bmatrix} \begin{bmatrix} R_{t_{sm}} \\ Q_{t_{sm}} \\ D_{t_{sm}} \end{bmatrix} + \begin{bmatrix} 0 & 0 \\ -0.1143 & 0.0001 \end{bmatrix} \begin{bmatrix} \zeta_{t_{sm}}^h \\ V \end{bmatrix}$$
(B.5)

Appendix C. Cost functions and parameters for the examples

For the CSTR cost functions used in Example 1 and 2, we use Eq. (22) to estimate the fixed design cost. The cost parameters a, b, and n are listed in Table C.1 for year 2010.

Table C.1

Example 1 - Reactor cost parameters for year 2010 (Towler and Sinnott, 2013).

J. 1015)	•
Parameter	Value
a	61,500
b	32,500
n	0.6

The cost estimation from 2010 is projected to 2018 by using Eq. (C.1) the Chemical Engineering Plant Cost Index (CEPCI) (che, 2018).

$$Cost_{2018} = Cost_{2010} \frac{CEPCI_{2018}}{CEPCI_{2010}}$$
 (C.1)

where the cost indexes $CEPCI_{2010}$ and $CEPCI_{2018}$ are 532.9 and 588.0, respectively.

For the CHP fixed cost estimation, on the other hand, we use a linear function, given in Eq. (C.2) (Diangelakis et al., 2017b)

$$Cost_{CHP} = 370 + 0.0857V_{CHP} \tag{C.2}$$

References

Alanqar, A., Durand, H., Albalawi, F., Christofides, P.D., 2017. An economic model predictive control approach to integrated production management and process operation. AlChe J. 63 (6), 1892–1906. doi:10.1002/aic.15553.

Amrit, R., Rawlings, J.B., Angeli, D., 2011. Economic optimization using model predictive control with a terminal cost. Annu. Rev. Control 35 (2), 178–186. doi:10.1016/j.arcontrol.2011.10.011.

Bahri, P., Bandoni, J., Romagnoli, J., 1997. Integrated flexibility and controllability analysis in design of chemical processes. AIChE J. 43 (4), 997–1015.

Baldea, M., Du, J., Park, J., Harjunkoski, I., 2015. Integrated production scheduling and model predictive control of continuous processes. AIChE J. 61 (12), 4179– 4190. doi:10.1002/aic.14951.

Baldea, M., Harjunkoski, I., 2014. Integrated production scheduling and process control: a systematic review. Comput. Chem. Eng. 71, 377–390. doi:10.1016/j. compchemeng.2014.09.002.

Bansal, V., Perkins, J., Pistikopoulos, E., 2002. A case study in simultaneous design and control using rigorous, mixed-integer dynamic optimization models. Ind. Eng. Chem. Res. 41 (4), 760–778.

Bansal, V., Perkins, J., Pistikopoulos, E., Ross, R., Van Schijndel, J., 2000a. Simultaneous design and control optimisation under uncertainty. Comput. Chem. Eng. 24 (2–7), 261–266. doi:10.1016/S0098-1354(00)00475-0.

Bansal, V., Ross, R., Perkins, J., Pistikopoulos, E., 2000b. Interactions of design and control: double-effect distillation. J. Process Control 10 (2), 219–227. doi:10. 1016/S0959-1524(99)00017-7.

Bansal, V., Sakizlis, V., Ross, R., Perkins, J., Pistikopoulos, E., 2003. New algorithms for mixed-integer dynamic optimization. Comput. Chem. Eng. 27 (5), 647–668. doi:10.1016/S0098-1354(02)00261-2.

Bassett, M., Dave, P., Doyle, F., Kudva, G., Pekny, J., Reklaitis, G., Subrahmanyam, S., Miller, D., Zentner, M., 1996. Perspectives on model based integration of process operations. Comput. Chem. Eng. 20 (6), 821–844. doi:10.1016/0098-1354(95) 00184-0

- Beal, L.D., Petersen, D., Grimsman, D., Warnick, S., Hedengren, J.D., 2018. Integrated scheduling and control in discrete-time with dynamic parameters and constraints. Comput. Chem. Eng. 115, 361–376. doi:10.1016/j.compchemeng.2018.04. 010
- Bemporad, A., Morari, M., Dua, V., Pistikopoulos, E.N., 2002. The explicit linear quadratic regulator for constrained systems. Automatica 38 (1), 3–20. doi:10. 1016/S0005-1098(01)00174-1.
- Brengel, D., Seider, W., 1992. Coordinated design and control optimization of nonlinear processes. Comput. Chem. Eng. 16 (9), 861–886. doi:10.1016/0098-1354(92) 80038-B.
- Burnak, B., Katz, J., Diangelakis, N.A., Pistikopoulos, E.N., 2018a. Integration of design, scheduling, and control of combined heat and power systems: a multiparametric programming based approach. In: Computer Aided Chemical Engineering, 44. Elsevier, pp. 2203–2208.
- Burnak, B., Katz, J., Diangelakis, N.A., Pistikopoulos, E.N., 2018b. Simultaneous process scheduling and control: a multiparametric programming-based approach. Ind. Eng. Chem. Res. 57 (11), 3963–3976. doi:10.1021/acs.iecr.7b04457.
- Capón-García, E., Guillén-Gosálbez, G., Espuña, A., 2013. Integrating process dynamics within batch process scheduling via mixed-integer dynamic optimization. Chem. Eng. Sci. 102, 139–150. doi:10.1016/j.ces.2013.07.039.
- Charitopoulos, V.M., Papageorgiou, L.G., Dua, V., 2018. Closed-loop integration of planning, scheduling and multi-parametric nonlinear control. Comput. Chem. Eng. doi:10.1016/j.compchemeng.2018.06.021.
- Chatrattanawet, N., Skogestad, S., Arpornwichanop, A., 2014. Control structure design and controllability analysis for solid oxide fuel cell. Chem. Eng. Trans. 39 (Special Issue), 1291–1296. doi:10.3303/CET1439216.
- Chatzidoukas, C., Perkins, J.D., Pistikopoulos, E.N., Kiparissides, C., 2003. Optimal grade transition and selection of closed-loop controllers in a gas-phase olefin polymerization fluidized bed reactor. Chem. Eng. Sci. 58 (0009), 3643–3658. doi:10.1016/S0009-2509(03)00223-9.
- Chen, Y., Adams, T., Barton, P., 2011a. Optimal design and operation of flexible energy polygeneration systems. Ind. Eng. Chem. Res. 50 (8), 4553–4566. doi:10.1021/ie1021267.
- Chen, Y., Adams, T., Barton, P., 2011b. Optimal design and operation of static energy polygeneration systems. Ind. Eng. Chem. Res. 50 (9), 5099–5113. doi:10.1021/ie101568v.
- Chu, Y., You, F., 2012. Integration of scheduling and control with online closed-loop implementation: fast computational strategy and large-scale global optimization algorithm. Comput. Chem. Eng. 47, 248–268. doi:10.1016/j.compchemeng.2012. 06.035.
- Chu, Y., You, F., 2013. Integration of production scheduling and dynamic optimization for multi-product CSTRs: generalized benders decomposition coupled with global mixed-integer fractional programming. Comput. Chem. Eng. 58, 315–333. doi:10.1016/j.compchemeng.2013.08.003.
- Chu, Y., You, F., 2015. Model-based integration of control and operations: overview, challenges, advances, and opportunities. Comput. Chem. Eng. 83, 2–20. doi:10. 1016/j.compchemeng.2015.04.011.
- Costandy, J.G., Edgar, T.F., Baldea, M., 2018. A scheduling perspective on the monetary value of improving process control. Comput. Chem. Eng. 112, 121–131. doi:10.1016/j.compchemeng.2018.01.019.
- Daoutidis, P., Lee, J.H., Harjunkoski, I., Skogestad, S., Baldea, M., Georgakis, C., 2018. Integrating operations and control: a perspective and roadmap for future research. Comput. Chem. Eng. 115, 179–184. doi:10.1016/j.compchemeng.2018.04.011
- De La Fuente, R.-N., Flores-Tlacuahuac, A., 2009. Integrated design and control using a simultaneous mixed-integer dynamic optimization approach. Ind. Eng. Chem. Res. 48 (4), 1933–1943. doi:10.1021/ie801353c.
- Diangelakis, N.A., Burnak, B., Pistikopoulos, E.N., 2017a. A multi-parametric programming approach for the simultaneous process scheduling and control Application to a domestic cogeneration unit. Foundations of Computer Aided Process Operations/Chemical Process Control (FOCAPO/CPC) http://folk.ntnu.no/skoge/prost/proceedings/focapo-cpc-2017/FOCAPO-CPC%202017%20Contributed %20Papers/72_FOCAPO_Contributed.pdf.
- Diangelakis, N., Panos, C., Pistikopoulos, E., 2014. Design optimization of an internal combustion engine powered CHP system for residential scale application. Comput. Manag. Sci. 11 (3), 237–266. doi:10.1007/s10287-014-0212-z.
- Diangelakis, N.A., Avraamidou, S., Pistikopoulos, E.N., 2016. Decentralized multiparametric model predictive control for domestic combined heat and power systems. Ind. Eng. Chem. Res. 55 (12), 3313–3326. doi:10.1021/acs.iecr. 5h03335
- Diangelakis, N.A., Burnak, B., Katz, J., Pistikopoulos, E.N., 2017b. Process design and control optimization: a simultaneous approach by multi-parametric programming. AlChE J. 63 (11), 4827–4846. doi:10.1002/aic.15825.
- Diangelakis, N.A., Pistikopoulos, E.N., 2017. A multi-scale energy systems engineering approach to residential combined heat and power systems. Comput. Chem. Eng. 102, 128–138. doi:10.1016/j.compchemeng.2016.10.015.
- Dias, L.S., Ierapetritou, M.G., 2016. Integration of scheduling and control under uncertainties: review and challenges. Chem. Eng. Res. Des. 116, 98–113. doi:10.1016/j.cherd.2016.10.047.
- Dias, L.S., lerapetritou, M.G., 2017. From process control to supply chain management: an overview of integrated decision making strategies. Comput. Chem. Eng. 106. 826–835. doi:10.1016/j.compchemeng.2017.02.006.
- Dias, L.S., Pattison, R.C., Tsay, C., Baldea, M., Ierapetritou, M.G., 2018. A simulation-based optimization framework for integrating scheduling and model predictive control, and its application to air separation units. Comput. Chem. Eng. 113, 139–151. doi:10.1016/j.compchemeng.2018.03.009.

- Du, J., Park, J., Harjunkoski, I., Baldea, M., 2015. A time scale-bridging approach for integrating production scheduling and process control. Comput. Chem. Eng. 79, 59–69. doi:10.1016/j.compchemeng.2015.04.026.
- Economic indicators. Chem. Eng. 125 (7), 64, 2018
- Ellis, M., Christofides, P.D., 2014a. Integrating dynamic economic optimization and model predictive control for optimal operation of nonlinear process systems. Control Eng. Pract. 22, 242–251. doi:10.1016/j.conengprac.2013.02.016.
- Ellis, M., Christofides, P.D., 2014b. Selection of control configurations for economic model predictive control systems. AlChE J. 60 (9), 3230–3242. doi:10.1002/aic. 14514
- Ellis, M., Christofides, P.D., 2015. Real-time economic model predictive control of nonlinear process systems. AlChE J. 61 (2), 555–571. doi:10.1002/aic.14673.
- Ellis, M., Durand, H., Christofides, P.D., 2014. A tutorial review of economic model predictive control methods. J. Process Control 24 (8), 1156–1178. doi:10.1016/j. jprocont.2014.03.010. Economic nonlinear model predictive control
- Engell, S., Harjunkoski, I., 2012. Optimal operation: scheduling, advanced control and their integration. Comput. Chem. Eng. 47, 121–133. doi:10.1016/j.compchemeng.2012.06.039.
- Flores-Tlacuahuac, A., Biegler, L., 2007. Simultaneous mixed-integer dynamic optimization for integrated design and control. Comput. Chem. Eng. 31 (5–6), 588–600. doi:10.1016/j.compchemeng.2006.08.010.
- Flores-Tlacuahuac, A., Biegler, L., 2008. Integrated control and process design during optimal polymer grade transition operations. Comput. Chem. Eng. 32 (11), 2823–2837. doi:10.1016/j.compchemeng.2007.12.005.
- Flores-Tlacuahuac, A., Grossmann, I.E., 2006. Simultaneous cyclic scheduling and control of a multiproduct CSTR. Ind. Eng. Chem. Res. 45 (20), 6698–6712. doi:10.1021/ie051293d.
- Flores-Tlacuahuac, A., Grossmann, I.E., 2010. Simultaneous cyclic scheduling and control of tubular reactors: single production lines. Ind. Eng. Chem. Res. 49, 11453–11463. doi:10.1021/ie1008629.
- Flores-Tlacuahuac, A., Grossmann, I.E., 2011. Simultaneous cyclic scheduling and control of tubular reactors: parallel production lines. Ind. Eng. Chem. Res. 50 (13), 8086–8096. doi:10.1021/ie101677e.
- Floudas, C., 2000. Global optimization in design and control of chemical process systems. J. Process Control 10 (2), 125–134. doi:10.1016/S0959-1524(99)00019-0.
- Floudas, C., Gümüş, Z., Ierapetritou, M., 2001. Global optimization in design under uncertainty: feasibility test and flexibility index problems. Ind. Eng. Chem. Res. 40 (20), 4267–4282.
- Georgiadis, M., Schenk, M., Pistikopoulos, E., Gani, R., 2002. The interactions of design, control and operability in reactive distillation systems. Comput. Chem. Eng. 26 (4–5), 735–746. doi:10.1016/S0098-1354(01)00774-8.
- Ghobeity, A., Mitsos, A., 2014. Optimal design and operation of desalination systems: new challenges and recent advances. Curr. Opin. Chem. Eng. 6, 61–68. doi:10.1016/j.coche.2014.09.008.
- Gong, J., Hytoft, G., Gani, R., 1995. An integrated computer aided system for integrated design and control of chemical processes. Comput. Chem. Eng. 19 (SUPPL. 1), 489–494. doi:10.1016/0098-1354(95)87084-9.
- Grossmann, I., 2005. Enterprise-wide optimization: a new frontier in process systems engineering. AlChE J. 51 (7), 1846–1857. doi:10.1002/aic.10617.
- Gutiérrez-Limón, M.A., Flores-Tlacuahuac, A., Grossmann, I.E., 2012. A multiobjective optimization approach for the simultaneous single line scheduling and control of CSTRs. Ind. Eng. Chem. Res. 51 (17), 5881–5890. doi:10.1021/ie201740s.
- Gutiérrez-Limón, M.A., Flores-Tlacuahuac, A., Grossmann, I.E., 2014. MINLP Formulation for simultaneous planning, scheduling, and control of short-period single-unit processing systems. Ind. Eng. Chem. Res. 53 (38), 14679–14694. doi:10.1021/ie402563j.
- Harjunkoski, I., Nyström, R., Horch, A., 2009. Integration of scheduling and control-Theory or practice? Comput. Chem. Eng. 33 (12), 1909–1918. doi:10.1016/j. compchemeng.2009.06.016.
- Huercio, A., Espuña, A., Puigjaner, L., 1995. Incorporating on-line scheduling strategies in integrated batch production control. Comput. Chem. Eng. 19 (SUPPL. 1), 609–614. doi:10.1016/0098-1354(95)87102-0.
- Jamaludin, M.Z., Swartz, C.L.E., 2017. Dynamic real-time optimization with closed-loop prediction. AlChE J. 63 (9), 3896–3911. doi:10.1002/aic.15752.
- Katz, J., Burnak, B., Pistikopoulos, E.N., 2018. The impact of model approximation in multiparametric model predictive control. Chem. Eng. Res. Des. 139, 211–223. doi:10.1016/j.cherd.2018.09.034.
- Kelley, M.T., Pattison, R.C., Baldick, R., Baldea, M., 2018. An efficient MILP framework for integrating nonlinear process dynamics and control in optimal production scheduling calculations. Comput. Chem. Eng. 110, 35–52. doi:10.1016/j.compchemeng.2017.11.021.
- Koller, R.W., Ricardez-Sandoval, L.A., Biegler, L.T., 2018. Stochastic back-off algorithm for simultaneous design, control, and scheduling of multiproduct systems under uncertainty. AIChE J. 64 (7), 2379–2389. doi:10.1002/aic.16092.
- Kookos, I., Perkins, J., 2002. An algorithmic method for the selection of multivariable process control structures. J. Process Control 12 (1), 85–99. doi:10.1016/S0959-1524(00)00063-9.
- Kookos, I., Perkins, J., 2016. Control structure selection based on economics: generalization of the back-off methodology. AlChE J. 62 (9), 3056–3064. doi:10.1002/aic.15284.
- Kopanos, G.M., Georgiadis, M.C., Pistikopoulos, E.N., 2013. Energy production planning of a network of micro combined heat and power generators. Appl. Energy 102, 1522–1534. doi:10.1016/j.apenergy.2012.09.015.
- Kopanos, G.M., Pistikopoulos, E.N., 2014. Reactive scheduling by a multiparametric programming rolling horizon framework: a case of a network of combined

- heat and power units. Ind. Eng. Chem. Res. 53 (11), 4366–4386. doi:10.1021/ie402393s.
- Li, X., Barton, P., 2015. Optimal design and operation of energy systems under uncertainty. J. Process Control 30, 1–9. doi:10.1016/j.jprocont.2014.11.004.
- Liu, S., Liu, J., 2016. Economic model predictive control with extended horizon. Automatica 73, 180–192. doi:10.1016/j.automatica.2016.06.027.
- Löfberg, J., 2004. Yalmip: a toolbox for modeling and optimization in MATLAB. In:
 Proceedings of the IEEE International Symposium on Computer-Aided Control
 System Design, pp. 284–289.
- Luyben, M., Floudas, C., 1994. Analyzing the interaction of design and control-1. a multiobjective framework and application to binary distillation synthesis. Comput. Chem. Eng. 18 (10), 933–969. doi:10.1016/0098-1354(94)
- Mahadevan, R., Doyle III, F.J., Allcock, A.C., 2002. Control-Relevant scheduling of polymer grade transitions. AlChE J. 48 (8), 1754–1764.
- Malcolm, A., Polan, J., Zhang, L., Ogunnaike, B., Linninger, A., 2007. Integrating systems design and control using dynamic flexibility analysis. AIChE J. 53 (8), 2048–2061. doi:10.1002/aic.11218.
- Mehta, S., Ricardez-Sandoval, L., 2016. Integration of design and control of dynamic systems under uncertainty: a new back-off approach. Ind. Eng. Chem. Res. 55 (2), 485–498. doi:10.1021/acs.iecr.5b03522.
- Mitra, K., Gudi, R.D., Patwardhan, S.C., Sardar, G., 2010. Resiliency issues in integration of scheduling and control. Ind. Eng. Chem. Res. 49 (1), 222–235. doi:10.1021/ie900380s.
- Mohideen, M., Perkins, J., Pistikopoulos, E., 1996. Optimal synthesis and design of dynamic systems under uncertainty. Comput. Chem. Eng. 20 (SUPPL.2), S895–S900.
- Mohideen, M., Perkins, J., Pistikopoulos, E., 1997. Robust stability considerations in optimal design of dynamic systems under uncertainty. J. Process Control 7 (5), 371–385.
- Narraway, L., Perkins, J., Barton, G., 1991. Interaction between process design and process control: economic analysis of process dynamics. J. Process Control 1 (5), 243–250. doi:10.1016/0959-1524(91)85015-B.
- Nie, Y., Biegler, L.T., Villa, C.M., Wassick, J.M., 2015. Discrete time formulation for the integration of scheduling and dynamic optimization. Ind. Eng. Chem. Res. 54 (16), 4303–4315. doi:10.1021/ie502960p.
- Nie, Y., Biegler, L.T., Wassick, J.M., 2012. Integrated scheduling and dynamic optimization of batch processes using state equipment networks. AIChE J. 58 (11), 3416–3432. doi:10.1002/aic.13738.
- Oberdieck, R., Diangelakis, N.A., Papathanasiou, M.M., Nascu, I., Pistikopoulos, E.N., 2016. POP Parametric Optimization toolbox. Ind. Eng. Chem. Res. 55 (33), 8979–8991. doi:10.1021/acs.iecr.6b01913.
- Papalexandri, K., Pistikopoulos, E., 1994. Synthesis and retrofit design of operable heat exchanger networks. 1.flexibility and structural controllability aspects. Ind. Eng. Chem. Res. 33 (7), 1718–1737.
- Patil, B.P., Maia, E., Ricardez-sandoval, L.A., 2015. Integration of scheduling, design, and control of multiproduct chemical processes under uncertainty. AIChE J. 61 (8), doi:10.1002/aic.
- Pattison, R.C., Touretzky, C.R., Johansson, T., Harjunkoski, I., Baldea, M., 2016. Optimal process operations in fast-Changing electricity markets: framework for scheduling with low-Order dynamic models and an air separation application. Ind. Eng. Chem. Res. 55 (16), 4562–4584. doi:10.1021/acs.iecr.5b03499.
- Pistikopoulos, E., lerapetritou, M., 1995. Novel approach for optimal process design under uncertainty. Comput. Chem. Eng. 19 (10), 1089–1110. doi:10.1016/0098-1354(94)00093-4.
- Pistikopoulos, E.N., Diangelakis, N.A., 2016. Towards the integration of process design, control and scheduling: are we getting closer? Comput. Chem. Eng. 91, 85–92. https://doi.org/10.1016/j.compchemeng.2015.11.002.
- Pistikopoulos, E.N., Diangelakis, N.A., Oberdieck, R., Papathanasiou, M.M., Nascu, I., Sun, M., 2015. PAROC-An Integrated framework and software platform for the optimisation and advanced model-based control of process systems. Chem. Eng. Sci. 136, 115–138. https://doi.org/10.1016/j.ces.2015.02.030.
- Qin, S., Badgwell, T.A., 2003. A survey of industrial model predictive control technology. Control Eng. Pract. 11 (7), 733–764. doi:10.1016/S0967-0661(02) 00186-7.
- Rafiei, M., Ricardez-Sandoval, L.A., 2018. Stochastic back-off approach for integration of design and control under uncertainty. Ind. Eng. Chem. Res. 57 (12), 4351–4365. doi:10.1021/acs.iecr.7b03935.

- Rafiei-Shishavan, M., Mehta, S., Ricardez-Sandoval, L., 2017. Simultaneous design and control under uncertainty: a back-off approach using power series expansions. Comput. Chem. Eng. 99, 66–81. doi:10.1016/j.compchemeng.2016.12.015.
- Ricardez-Sandoval, L., 2011. Current challenges in the design and control of multiscale systems. Can. J. Chem. Eng. 89 (6), 1324–1341. doi:10.1002/cjce.20607.
- Ricardez-Sandoval, L., 2012a. Optimal design and control of dynamic systems under uncertainty: a probabilistic approach. Comput. Chem. Eng. 43, 91–107. doi:10. 1016/j.compchemeng.2012.03.015.
- Ricardez-Sandoval, L., Budman, H., Douglas, P., 2008. Simultaneous design and control of processes under uncertainty: a robust modelling approach. J. Process Control 18 (7–8), 735–752. doi:10.1016/j.jprocont.2007.11.006.
- Ricardez-Sandoval, L., Budman, H., Douglas, P., 2009. Integration of design and control for chemical processes: a review of the literature and some recent results. Annu. Rev. Control 33 (2), 158–171. doi:10.1016/j.arcontrol.2009.06.001.
- Ricardez-Sandoval, L.A., 2012b. Optimal design and control of dynamic systems under uncertainty: a probabilistic approach. Comput. Chem. Eng. 43, 91–107. doi:10.1016/j.compchemeng.2012.03.015.
- Sakizlis, V., Perkins, J., Pistikopoulos, E., 2003. Parametric controllers in simultaneous process and control design optimization. Ind. Eng. Chem. Res. 42 (20), 4545–4563
- Sakizlis, V., Perkins, J., Pistikopoulos, E., 2004. Recent advances in optimization-based simultaneous process and control design. Comput. Chem. Eng. 28 (10), 2069–2086. doi:10.1016/j.compchemeng.2004.03.018.
- Soroush, M., Kravaris, C., 1993a. Optimal design and operation of batch reactors. 1. theoretical framework. Ind. Eng. Chem. Res. 32 (5), 866–881.
- Soroush, M., Kravaris, C., 1993b. Optimal design and operation of batch reactors. 2. a case study. Ind. Eng. Chem. Res. 32 (5), 882–893.
- Subramanian, K., Maravelias, C.T., Rawlings, J.B., 2012. A state-space model for chemical production scheduling. Comput. Chem. Eng. 47, 97–110. doi:10.1016/ j.compchemeng.2012.06.025.
- Subramanian, K., Rawlings, J.B., Maravelias, C.T., Flores-Cerrillo, J., Megan, L., 2013. Integration of control theory and scheduling methods for supply chain management. Comput. Chem. Eng. 51, 4–20. doi:10.1016/j.compchemeng.2012.06.012.
- Terrazas-Moreno, S., Flores-Tlacuahuac, A., Grossmann, I.E., 2007. Simultaneous cyclic scheduling and optimal control of polymerization reactors. AlChE J. 53 (9), 2301–2315. doi:10.1002/aic.11247.
- Terrazas-Moreno, S., Flores-Tlacuahuac, A., Grossmann, I.E., 2008. Simultaneous design, scheduling, and optimal control of a methyl-methacrylate continuous polymerization reactor. AlChE J. 54 (12), 3160–3170. doi:10.1002/aic.11658.
- Touretzky, C.R., Baldea, M., 2014. Integrating scheduling and control for economic MPC of buildings with energy storage. J. Process Control 24 (8), 1292–1300. doi:10.1016/j.jprocont.2014.04.015. Economic nonlinear model predictive control
- Towler, G., Sinnott, R., 2013. Chapter 7 capital cost estimating. In: Towler, G., Sinnott, R. (Eds.), Chemical Engineering Design. Butterworth-Heinemann, Boston, pp. 307–354. doi:10.1016/B978-0-08-096659-5.00007-9.
- Vega, P., Lamanna, R., Revollar, S., Francisco, M., 2014a. Integrated design and control of chemical processes - part ii: an illustrative example. Comput. Chem. Eng. 71, 618–635. doi:10.1016/j.compchemeng.2014.09.019.
- Vega, P., Lamanna de Rocco, R., Revollar, S., Francisco, M., 2014b. Integrated design and control of chemical processes - part i: revision and classification. Comput. Chem. Eng. 71, 602–617. doi:10.1016/j.compchemeng.2014.05.010.
- Washington, I., Swartz, C., 2014. Design under uncertainty using parallel multiperiod dynamic optimization. AIChE J. 60 (9), 3151–3168. doi:10.1002/aic.14473.
- Würth, L., Hannemann, R., Marquardt, W., 2011. A two-layer architecture for economically optimal process control and operation. J. Process Control 21 (3), 311–321. doi:10.1016/j.jprocont.2010.12.008.
- Yuan, Z., Chen, B., Sin, G., Gani, R., 2012. State-of-the-art and progress in the optimization-based simultaneous design and control for chemical processes. AlChE J. 58 (6), 1640–1659. doi:10.1002/aic.13786.
- Zhang, L., Xue, C., Malcolm, A., Kulkarni, K., Linninger, A., 2006. Distributed system design under uncertainty. Ind. Eng. Chem. Res. 45 (25), 8352–8360. doi:10.1021/ icoconst.
- Zhuge, J., Ierapetritou, M.G., 2012. Integration of scheduling and control with closed loop implementation. Ind. Eng. Chem. Res. 51 (25), 8550–8565. doi:10.1021/ io2002364
- Zhuge, J., Ierapetritou, M.G., 2014. Integration of scheduling and control for batch processes using multi-parametric model predictive control. AIChE J. 60 (9), 3169–3183. doi:10.1002/aic.14509.